GUIDANCE DOCUMENTS ON MEASUREMENTS & MODELLING OF NOVEL AIR QUALITY POLLUTANTS:

SOURCE APPORTIONMENT TECHNIQUES FOR PARTICULATE MATTER

RI-URBANS

Research Infrastructures Services Reinforcing Air Quality Monitoring Capacities in European Urban & Industrial AreaS (GA n. 101036245)

By

05/11/2024

RI-URBANS (http://www.RIURBANS.eu) is supported by the European Commission under the Horizon 2020 – Research and Innovation Framework Programme, H2020-GD-2020, Grant Agreement number: 101036245

Authors: Fulvio Amato (CSIC), Marta Via (CSIC), Mannos Manousakas (PSI), Benjamin Chazeau (AMU), Gang Chen (ICL), Barend L. van Drooge (CSIC), Jean-Luc Jaffrezo (University of Grenoble, UGA), Olivier Favez (INERIS), Cristina Colombi (ARPA Lombardia), Eleonora Cuccia (ARPA Lombardia), Guido Lanzani (ARPA Lombardia), André S.H. Prevot (PSI), Andrés Alastuey (CSIC) & Xavier Querol (CSIC)

Rewievers: J. Eudes Petit (CNRS), Katriina Kyllönen (FMI), Hilkka Timonen (FMI), Anja Tremper (ICL), Elli Suhonen (FMI)

RI-URBANS (http://www.RIURBANS.eu) is supported by the European Commission under the Horizon 2020 – Research and Innovation Framework Programme, H2020-GD-2020, Grant Agreement number: 101036245

Table of Contents

ABBREVIATIONS ..... **I**

CHEMICAL SYMBOLS ..... **II**

1. ABOUT THIS DOCUMENT **1**

2. SOURCE APPORTIONMENT BASED ON 24H RESOLUTION PM CHEMISTRY DATA **1**

2.1. GUIDELINES FOR IMPLEMENTING POSITIVE MATRIX FACTORISATION ANALYSES 1
2.2. RI-URBANS'S PMF SENSITIVITY ANALYSIS OF THE NEED OF SPECIFIC TRACERS OF SOURCES 2
2.4 DISCUSSION OF THE RESULTS 11
2.5 RECOMMENDATIONS FOR OFF-LINE SOURCE APPORTIONMENT BASED ON 24H RESOLUTION PM CHEMISTRY DATA 12

3. SOURCE APPORTIONMENT BASED ON HIGH-TIME RESOLUTION ORGANIC AEROSOL MEASUREMENTS **13**

3.1. METHODOLOGY 13
3.2. PAN-EUROPEAN OVERVIEW OF SOURCE APPORTIONMENT 14
3.2.1 Methodology *14*
3.2.2 Pan-European overview of results *15*
3.3 RECOMMENDATIONS FOR OFFLINE SOURCE APPORTIONMENT BASED ON ORGANIC AEROSOL MEASUREMENTS OF HIGH TIME RESOLUTION 18

4. SOURCE APPORTIONMENT BASED ON HIGH TIME RESOLUTION TRACE ELEMENTS MEASUREMENTS **19**

4.1 METHODOLOGY 19
4.2 PAN-EUROPEAN OVERVIEW OF SOURCE APPORTIONMENT 20
4.3 RECOMMENDATIONS FOR SOURCE APPORTIONMENT BASED ON HIGH TIME RESOLUTION MEASUREMENTS OF TRACE ELEMENTS 22

5. SOURCE APPORTIONMENT BASED ON DATASETS WITH DIFFERENT TIME-RESOLUTION **24**

5.1 METHODOLOGY 24
5.2 RECOMMENDATIONS FOR SOURCE APPORTIONMENT BASED ON COMBINED DATASETS 24

7. REFERENCES AND OTHER USEFUL LITERATURE **25**

ABBREVIATIONS

ACSM	Aerosol chemical speciation monitor
ACTRIS	Aerosols, Clouds and Trace gases Research InfraStructure
AMS	Aerosol mass spectrometry
BB	Biomass burning
BBOA	Biomass burning organic aerosols
BC	Black carbon
CMB	Chemical balance model
COA	Cooking-like organic aerosols
CSOA	Cigarette-smoke organic aerosols
DL	Detection limit
DW	Downweight
EC	Elemental carbon
EI-MS	Electron impact mass spectrometry
EUSAAR	European Supersites for Atmospheric Aerosol Research
GS-MS	Gas chromatography mass spectrometry
GC/NICI	Negative ion chemical ionization gas chromatography
HFO	Heavy fuel oil combustion
HOA	Hydrocarbon like organic aerosols
HPLC	High performance liquid chromography
HULIS	Humic-like substances
IC	Ion chromatography
ICP-MS	Inductively coupled plasma mass spectrometry
LC-PAD	Liquid chromatography with photodiode array detection
LO-OOA	Less-oxidised oxygenated organic aerosols
LOA	Local organic aerosols
MBTCA	1,2,3-butanetricarboxylic acid
MO-OOA	More-oxidised oxygenated organic aerosols
MS	Mass spectrometry
MTR	Multi-time resolution
NR-PM_1	Non-refractory PM_1
OA	Organic aerosols
OC	Organic carbon
OOA	Oxygenated organic aerosols
OP	Oxidative potential
PAD	Pulsed amperometric detection
PAH	Polyaromatic hydrocarbon
PM	Particulate matter
PM_1	Mass concentration of particles <1 µm
$PM_{2.5}$	Mass concentration of particles <2.5 µm
PM_{10}	Mass concentration of particles <10 µm
PMF	Positive Matrix Factorization, a receptor model for source apportionment
POA	Primary organic aerosol
Q-ACSM	Quadrupole aerosol chemical speciation monitor
RB	Regional background
RI-URBANS	Research Infrastructures Services Reinforcing Air Quality Monitoring Capacities in
S/N	Signal-to-noise ratio
SA	Source apportionment
SFC	Solid fuel combustion
ShINDOA	Shipping and industry organic aerosols
SIA	Secondary inorganic aerosol
SOA	Secondary organic aerosols
SU/SUB	Sub-urban background
ToF-ACSM	Time of flight aerosol chemical speciation monitor
TR	Traffic
UB	Urban background
UPLC	Ultra performance liquid chromatography
US-EPA	United States Environmental Protection Agency
VOC	Volatile organic compound
XRF	X-ray fluorescence

CHEMICAL SYMBOLS

Al	Aluminium
As	Arsenic
Ba	Barium
Br	Bromine
$C_2O_4^{2-}$	Oxalate
Ca	Calcium
Cd	Cadmium
Cl	Chlorine
Cr	Chromium
Cu	Copper
DHOPA	2,3-dihydroxy-4-oxopentanoic acid
Fe	Iron
HF	Hydrogen fluoride
HNO_3	Nitric acid
$HClO_4$	Perchloric acid
K	Potassium
La	Lanthanum
Li	Lithium
Mg	Magnesium
Mn	Manganese
MSA	Methanesulfonic acid
Na	Sodium
NH_3	Ammonia
NH_4	Ammonium
Ni	Nickel
NO	Nitrogen monoxide
NO_2	Nitrogen dioxide
NO_3	Nitrate
Pb	Lead
Rb	Rubidium
S	Sulfur
Sb	Antimony
Si	Silicon
Sn	Tin
SO_2	Sulphur dioxide
SO_4	Sulfate
Sr	Strontium
Ti	Titanium
V	Vanadium
Zn	Zinc
Zr	Zirconium

1. ABOUT THIS DOCUMENT

Source apportionment (SA) is a common modelling exercise aimed at identifying sources of pollutants. It is often used to estimate source contributions of particulate matter (PM) levels in ambient air.

Among the diverse SA techniques, receptor models are based on the measurements of multiple PM components to identify the main factors/sources responsible for their variations.

Positive Matrix Factorization (PMF) is the most widely used receptor model. It uses as inputs PM chemical characterization datasets (and related uncertainties), obtained either off-line (laboratory chemical characterization of PM_{10}, $PM_{2.5}$ or PM_1 samples collected on filters, generally with 24h resolution) or on-line (for real-time non-refractory submicrometric aerosol or elements, with high time resolution) or the combination of both (multi-time PMF).

The present document offers an overview of state-of-the-art procedures to conduct PMF analyses for the source apportionment of PM, as well as submicron organic aerosols (OA, the major fraction of fine aerosols) and trace elements (which are good tracers for a wide variety of PM sources). This made up the guidance document of the RI-URBANS service tools (ST) number 10 (ST10). It is worth mentioning that there is an additional guidance document (ST11) on the source apportionment of online measurement data of ultrafine particles-particle number size distribution (UFP-PNSD), black carbon (BC), online non-refractory PM speciation and volatile organic compounds (VOCs), as well as oxidative potential (OP).

This is a RI-URBANS/ACTRIS guidance for this specific service tool that is part of the RI-URBANS deliverable D46 (D6.1, containing guidance for all service tools provided in the project) with the support for publication from AXA Research Fund to build up the final dissemination D55 (D7.6). Any dissemination of results must indicate that it reflects only the author's view and that the European Commission is not responsible for any use that may be made of the information it contains.

2. SOURCE APPORTIONMENT BASED ON 24h RESOLUTION PM CHEMISTRY DATA

2.1. Guidelines for implementing positive matrix factorisation analyses

For the scope of this section, the recommended receptor model choice is PMF, which can be applied by means of the free US-EPA version 5 (https://www.epa.gov/air-research/positive-matrix-factorization-model-environmental-data-analyses). To optimize the PMF analysis and evaluate its performance we refer to two main documents:

- European Guide on Air Pollution Source Apportionment with Receptor Models (https://publications.jrc.ec.europa.eu/repository/handle/JRC117306)
- CEN/TS 17458:2020 Ambient Air - Methodology to Assess the Performance of Receptor Oriented Source Apportionment Modelling Applications for Particulate Matter.

In addition to these general guidelines, this section provides technical recommendations on the choice of chemical components to be used as input for PMF SA analysis.

In PMF, given that the different factors/sources are identified by means of their chemical profiles, the choice of chemical analyses to be performed prior to the PMF analysis is of crucial importance. During the last decades, a large body of literature has aimed to identify the most appropriate tracers for specific sources. For example, Cu, Sb, Sn, Ba, and Fe, among others, have been linked to brake wear emissions, Zn to tyre wear emissions, Pb, Mn, Zn and Cd to metallurgy, and V and Ni to shipping emissions (Amato et al., 2009). For the organic fraction, polyaromatic

hydrocarbons (PAHs) are associated mostly to primary combustion products, polyols to plant debris, levoglucosan, mannosan and galactosan to biomass combustion and several other molecular markers for biogenic and anthropogenic secondary aerosols (Srivastava et al., 2018). However, the choice of chemical analyses of PM samples depends on many different factors beside their suitability as tracers, such as available laboratory instrumentation and standards, filter material, budget limitation and sample mass limitation. In addition, there is no standard procedure to select the most appropriate components neither specific recommendations on this direction. This generates uncertainty in SA outputs not only in terms of number of sources identified but also, and consequently, in the source contributions estimates. In fact, PMF tends to reproduce most of the PM mass, regardless of the percentage of PM mass which has been chemically characterized, so that the lack of one specific source tracer (e.g. levoglucosan) can potentially affect the whole SA study. Sensitivity tests are limited in literature and aimed to investigate the influence of heavy-pollution days (e.g. desert dust outbreaks) time resolution, meteorological period, peak episode and interpolation method, showing an impact on source contributions up to 16 % of change. Additional sensitivity analyses showed that excluding some dates or reducing the associated temporal resolution (from 12h to 24h) retrieved fewer source factors and increased the errors of source contribution estimates. Considering the input variables, Cesari et al. (2016) performed separate tests on complete datasets (using the full range of available chemical species) and incomplete datasets (with reduced number of chemical species) showing that the profiles and the contributions of the different sources calculated with PMF were comparable within the estimated uncertainties indicating a good stability and robustness of PMF results. However, the study from Cesari et al. (2016) was performed only on inorganic PM speciation datasets and the choice of excluded components was aleatory.

2.2. RI-URBANS's PMF sensitivity analysis of the need of specific tracers of sources

This study evaluates quantitatively the impact of lacking tracers of specific sources on the whole SA, both in terms of identified sources and source contributions, with the aim of providing first recommendations on the most suitable and critical components to be included in the PMF analyses in order to reduce PMF output uncertainty as much as possible. To this aim we performed three sensitivity analyses on three different datasets across EU in order to cover different types of climatic (mediterranean, continental and alpine), urban conditions, source types and PM fractions.

In the framework of the RI-URBANS, we compiled existing European PM speciation datasets at urban background locations and selected three of them for the purpose of this study. The main selection criteria were: i) at least 1 year of measurements; ii) at least 120 samples; iii) presence of both organic and inorganic components. The three datasets were from:

- Barcelona (Spain), including an urban background air quality station (Palau Reial) and a traffic site (Eixample). The city of Barcelona lies along the western coast of the Mediterranean Basin, and it is delimited by two river basins (Besòs in the North and Llobregat in the South) and a forest mountain range in the West. The city is densely populated (15.880 inhabitants/km^2) counting 1.6 million inhabitants which doubles when the whole metropolitan area is considered (36 municipalities). The city suffers poor air quality in terms of particulate matter and NO_2, mostly due to road traffic emissions, although other significant contributions to PM levels are originated from industries, harbour and urban works (Amato et al., 2016). No significant impact of residential heating has been historically observed. The urban background sampling site is located in the University Campus area, 250 m away from one of the main roads in the city, while the traffic site is located on a busy road uphill with an average traffic volume of 80,000 vehicles/day. PM_{10} and PM_1 samples were collected on quartz filters during three different campaigns in 2010, 2019 and 2021, collecting a total of 440 samples. Merging datasets obtained in distant periods in the PMF analysis may produce bias due to the possible variation in chemical profile of PM sources. However, given that the 2010 campaign consisted of >100 samples separated between day and night we decided to include them in the analysis as it is known that samples with high contrast of source contributions improve significantly the PMF results (Norris et al., 2014). A fraction of each filter was acid

digested (5 mL HF, 2.5 mL HNO_3, 2.5 mL $HClO_4$) for the determination of major and trace elements (Querol et al., 2001) (Table 1); another fraction was leached for the determination of water-soluble ions by ion chromatography (IC), using 20 mL of MilliQ water (with an ultrasonic bath for 30 min); another fraction was used for determination of organic carbon (OC) and elemental carbon (EC) by thermal–optical analysis with the EUSAAR2 temperature program (Cavalli et al., 2010) by means of Sunset analysers. Organic components, namely, polycyclic aromatic hydrocarbons (PAHs), sugars, anhydro-sugars, hopanes, acids, and polyols were analysed by means of GC-MS (Alier et al., 2013; Fontal et al., 2015).

- Grenoble (France), including an urban background air quality station (Les Frênes). The city, surrounded by three mountain ranges, is considered the most densely populated area (160,000 inhabitants) of the French Alps. In addition to the urbanized area, forests, including both deciduous and coniferous species, and agriculture areas (pastures) dominate the land cover around Grenoble. This region experiences frequent severe PM pollution events in the winter due to the formation of thermal inversion layers that may promote pollutant accumulation (Bessagnet et al., 2020). Previous PMF studies have shown that residential heating, mainly biomass burning, accounts for a major fraction of PM in the winter, but that many other sources are also important for the composition of PM (Favez et al., 2010; Srivastava et al., 2018; Weber et al., 2019; Borlaza et al., 2021). Traffic and industrial activities contribute significantly to the observed PM concentration levels in Grenoble (Polo-Rehn et al., 2014), and primary and secondary biogenic organic aerosol are also largely present in the PM_{10} (Samake et al., 2019). The current study focuses on the PM_{10} samples (Tissu-quartz, Pallflex, Ø = 150 mm) collected every third day for one year (2013) using high volume samplers (DA-80, Digitel; sampling duration of 24 h at 30 m^3 h^{-1}). Overall, approximately 194 species were quantified in each sample. EC/OC was measured using a Sunset lab analyzer using the EUSAAR-2 thermal protocol (Cavalli et al., 2010). Humic-like substances (HULIS) were analysed following the protocol described by Baduel et al. (2010). Anions (Cl^-, NO_3^-, SO_4^{2-}), cations (NH_4^+, Ca^{2+}, Na^+, Mg^{2+}, K^+), methanesulfonic acid (MSA) and oxalate ($C_2O_4^{2-}$) were analysed by ion chromatography (Jaffrezo et al., 2005). Thirty-four metals and trace elements were quantified by ICP-MS (Alleman et al., 2010). Cellulose combustion markers (levoglucosan, mannosan and galactosan from biomass burning), three polyols (arabitol, sorbitol and mannitol) and glucose were quantified using HPLC-PAD (Piot et al., 2012). Twenty-one PAHs, 27 oxy-PAHs, and 32 nitro-PAHs were quantified using UPLC/UV-Fluorescence and Negative ion chemical ionization gas chromatography GC/NICI (Srivastava et al., 2018; Albinet et al., 2006; Albinet et al., 2014; Albinet et al., 2013; Tomaz et al., 2016). Twenty-seven higher alkanes (C13–C39), 10 hopanes, pristane, phytane, five sulfur containing PAHs, five lignin combustion markers (e.g., vanillin and coniferaldehyde) (Golly et al., 2015) and 11 compounds usually recognized as SOA markers (e.g., α-methylglyceric acid, pinic acid, methyl-nitrocatechols) (Nozière et al., 2015) were analysed by GC/EI-MS. The quantification of all SOA markers was performed using authentic standards.
- Milan (Italy), including one urban background air quality station (Pascal). Milan, and the Po Valley area in general, experience one of the worst air quality situations across Europe due to high anthropogenic emissions of primary PM but also of gaseous precursors (mostly NH_3) from the agricultural sector provoking high formation of secondary aerosols. The station is part of the ARPA Lombardia Air Quality Network, and it is one of the Italian supersites. It is located on the eastern side of Milan, the University area called Città Studi, in a playground about 130 m from the road traffic. PM_{10} and $PM_{2.5}$ samples were collected during 2017–2019 on Teflon (Pall), mixed cellulose ester (MCE, Advantec) and quartz microfibre filters (Pall, 47 mm diameter), with low-volume US-EPA reference method samplers (TECORA). Metals, EC/OC, ions and anhydrosugars were analysed by X-ray fluorescence (XRF), thermo-optical analysis and ion chromatography, respectively (Amato et al., 2016).

Once the base solution was definitively selected, (without any further addition of constraints on these base cases), the sensitivity analysis was based on a "brute force" approach, by excluding families of analytes, one at a time. A family of analytes is defined as the group of analytes which are determined by the same laboratory technique (e.g. X-ray fluorescence or ion chromatography), in order to mimic choices of input data that would be resulting from

availability of the chemical technique. Therefore, for each dataset, we obtained a number of *N* solutions where *N* is the number of families of analytes. *N* is equal to 8, 7, and 5 for Grenoble, Barcelona, and Milan, respectively (Tables 2, 3, 4). Each solution was compared with the base solution to identify the impact of excluding that specific family of analytes on the number/type of factors (*f*) and on the source contribution (*g*).

Table 1. *Description of the input data used for three PMF base solutions, and classification into strong and weak variables based on S/N ratio. *A seed value is required in the EPA PMF software as the starting point of iteration.*

Site	Para-meter	Years	Station type	Strong components	Weak components	Seed value*	Number of runs	Additional uncertainty
Barcelona (Spain)	PM_{10}, PM_1	2010, 2019, 2021	Urban back-ground Traffic	PM, Al, Ca, Fe, K, Mg, Na, S, Li, Mn, Ti, V, Cr, Co, Ni, Cu, Zn, As, Rb, Sr, Zr, Cd, Sn, Sb, La, Pb, Ba, OC, EC, NO_3^-, Cl, NH_4^+, succinic acid, glutaric acid, phthalic acid, cis-pinonic acid, malic acid, 3-hydroxyglutaric acid, methylbutanetricarboxylic acid (MBTCA), 2-methylglyceric acid, galactosan, mannosan, levoglucosan, benzanthracene, chrysene, benzo(b+j+k)fluoranthene, benzo(e)pyrene, benzo(a)pyrene, benzo[ghi]perylene	azealic acid, 2-methylthreitol, 2-methylerythritol, 17a(H)21β(H)-29-norhopane, 17a(H)21β(H)-hopane	23	10	10
Milan (Italy)	PM_{10}	2017–2019	Urban back-ground	Al, Si, Cl, K, Ca, Ti, Fe, Cu, Zn, Pb, OC, EC, NO_3^-, SO_4^{2-}, NH_4^+, Levoglucosan	Mn, Ni, Br, PM_{10}	38	20	10
Grenoble (France)	PM_{10}	2013	Urban back-ground	OC, EC, HULIS, Na^+, NH_4^+, Mg^{2+}, Cl^-, NO_3^-, SO_4^{2-}, Levoglucosan, Arabitol, Sorbitol, Benzo[a]pyrene, Benzo[g,h,i]perylene, In.[1,2,3-cd]pyrene, Coronene, Acenaphthenequinone, 6H-Dibenzo[b,d]Pyran-6-one, 1,8-Naphthalic anhydride, 1-Nitropyrene, Ba, Cu, Pb, Sb, Ti, Zn, Cr, V, Al, Ca, Fe, C27, C29, C31, C33, HP6, HP7, Coniferylaldehyde, Vanillic acid, Alpha-methyl glyceric acid, DHOPA, 3-Hydroxyglutaric Acid, Phthalic Acid, 2-Methyl erythritol	PM_{10}, HP5, HP8	55	20	5

In Figures 1 to 6, the uncertainty intervals due to the choice of input chemical components are plotted, for each source, versus the reference solution (base case). Such intervals do not include those cases in which that specific source is not identified, which would deliver a null contribution. For Barcelona, the plots are made separately for the urban and the traffic sites, and for the PM_{10} and PM_1. The following discussion is organized according to the type of sources of PM.

Primary traffic: This factor was almost always found in Grenoble, regardless of which family of analytes was excluded, since it is traced by two family of analytes: EC (with OC/EC ratio lower than 1) and elements such as Ba, Cu, and Sb (among others). However, when elements' family was excluded, this factor was merged with the Fungal spores factor, thus hampering the separation of the two sources contributions. The sensitivity analysis revealed a symmetric interval error in Grenoble for Primary traffic source contributions (±28% compared to the base case solution) when a family of analytes was excluded.

Vehicle exhaust: In contrast to Grenoble, the total traffic contribution was separated in two main factors in Barcelona and Milan: the vehicle exhaust and the vehicle non-exhaust factors. In Milan, the exhaust factor was

mostly of primary origin as it was traced by Zn and an OC/EC ratio of 1 and it was always found, regardless of the input components chosen. The interval error of Vehicle exhaust source contributions was also symmetric in Milan (±15%) when a family of analytes is excluded, except in the case that elements are excluded provoking a merging of exhaust and non-exhaust contributions in one factor with also an overestimation of this exhaust + non-exhaust contributions (13.6 µg/m^3 vs. 7.3 µg/m^3) compared to the reference solution. In Barcelona, it was traced by several PAHs and hopanes (17a(H)21β(H)-29-norhopane, 17a(H)21β(H)-hopane, benzo(a)anthracene, chrysene, benzo(b+j+k)fluoranthene, benzo(e)pyrene, benzo(a)pyrene and benzo[ghi]perylene) and EC as well as an OC/EC ratio of 1.93 indicating the inclusion of some SOA. This factor was always found except when non-polar organics (PAHs) were excluded.

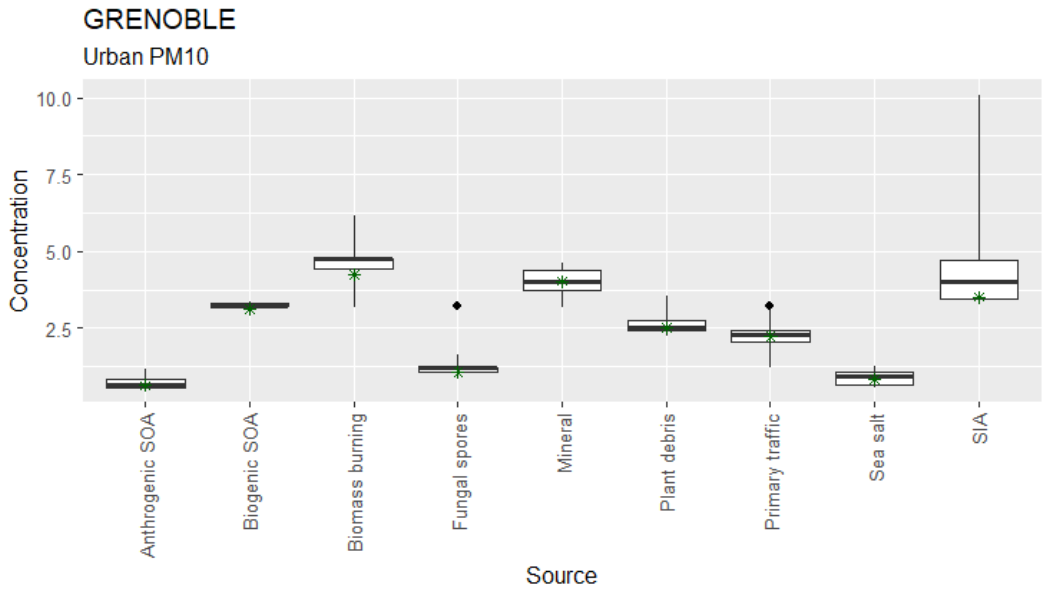

Figure 1. *Uncertainty intervals of PMF source contributions (µg/m^3) in Grenoble urban PM$_{10}$ due to the exclusion of different families of analytes. The case(s) in which a factor is not identified is not presented (i.e. null contribution). Stars indicate the base reference solution. Dots indicate fusions of factors. Adopted from Amato et al. (2024).*

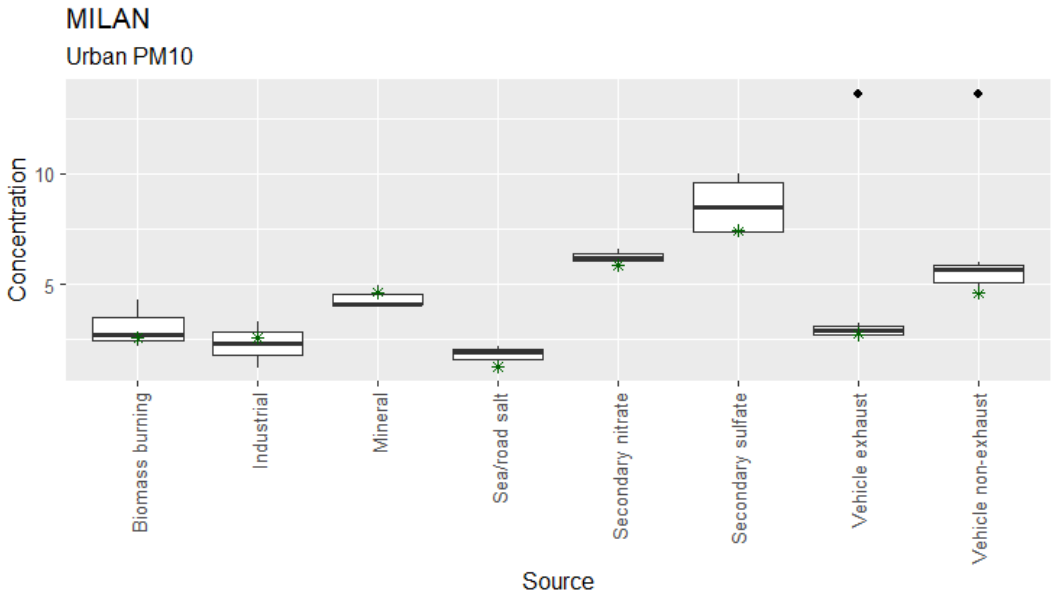

Figure 2. *Uncertainty intervals of PMF source contributions (µg/m^3) in Milan urban PM$_{10}$ due to the exclusion of different families of analytes. The case(s) in which a factor is not identified is not presented (i.e. null contribution). Stars indicate the base reference solution. Dots indicate fusions of factors. Adopted from Amato et al. (2024).*

In Barcelona urban PM_{10}, we observed an asymmetric interval with a more likely underestimation (-44%) of exhaust source contributions when families of analytes are excluded. When non-polar organics are excluded, we observed a merging of exhaust and non-exhaust contributions in one factor but with an underestimation of total contribution (5.8 µg/m^3 vs. 8.8 µg/m^3). For urban PM_1, the figure was similar but the underestimation of exhaust + non-exhaust contributions, when non-polar organics were excluded, was even more important (0.4 µg/m^3 vs. 3.9 µg/m^3). In the Barcelona traffic site, we observed a systematic overestimation (up to 3.5 and 2.5 times for PM_{10} and PM_1, respectively) when some analytes were excluded.

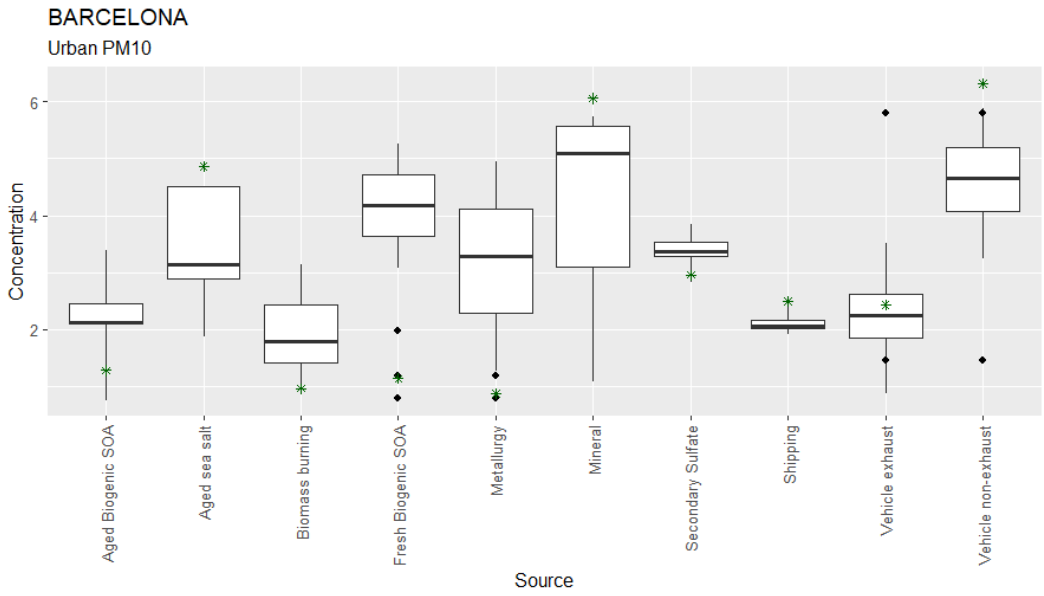

***Figure 3**. Uncertainty intervals of PMF source contributions (µg/m^3) in Barcelona urban PM_{10} due to the exclusion of different families of analytes. The case(s) in which a factor is not identified is not presented (i.e. null contribution). Stars indicate the base reference solution. Dots indicate fusions of factors. Adopted from Amato et al. (2024).*

Vehicle non-exhaust: The non-exhaust fraction of vehicle emissions was traced in both Barcelona and Milan by heavy metals and metalloids such as Cu, Sb, Sn, Ba, Fe, Cr and EC with an OC/EC ratio of 2.2 in Barcelona, and Cu, Fe, Pb and EC with an OC/EC ratio of 2.3 in Milan. In both cities, this factor was found except when elements were excluded from the PMF analysis, yielding to a unique traffic factor, as already mentioned earlier. For Barcelona, removing non-polar organics also provoked the loss of separation between exhaust and non-exhaust source contributions. The interval error of Vehicle non-exhaust source contributions revealed a systematic underestimation in Barcelona for PM_{10} at the traffic and background sites (down to 50%) when a family of analytes was excluded except in the case that ion chromatography was excluded provoking an overestimation (45%) of non-exhaust contributions. In Milan, instead, we observed a generic overestimation (up to 30%) of the *N* solutions excluding families of components.

Biomass burning: We observed very different outcomes from the sensitivity analyses in the three cities. In Milan and Barcelona, levoglucosan was crucial to identify biomass burning (BB) contributions in spite of the presence of PAHs in Barcelona. On the contrary, in the case of Grenoble, even discarding levoglucosan, the presence of PAHs allowed identifying the BB factor, as confirmed by the high correlation between the two source profiles, mostly for the concentrations of tracers such as EC, OC and PAHs. In Milan and Barcelona, the uncertainty due to the different

input components selection was estimated in a generic underestimation (up to a factor 2) of biomass burning source contributions, both in PM_{10} and PM_1 fractions, at both urban background and traffic sites.

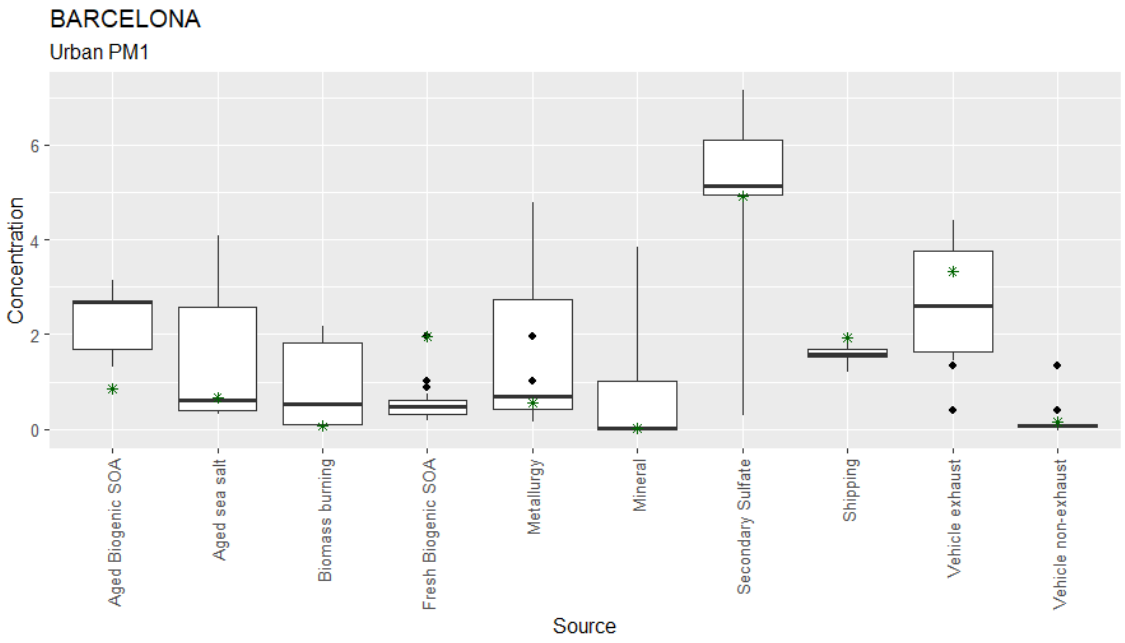

Figure 4. *Uncertainty intervals of PMF source contributions (µg/m³) in Barcelona urban PM_1 due to the exclusion of different families of analytes. The case(s) in which a factor is not identified is not presented (i.e. null contribution). Stars indicate the base reference solution. Dots indicate fusions of factors. Adopted from Amato et al. (2024).*

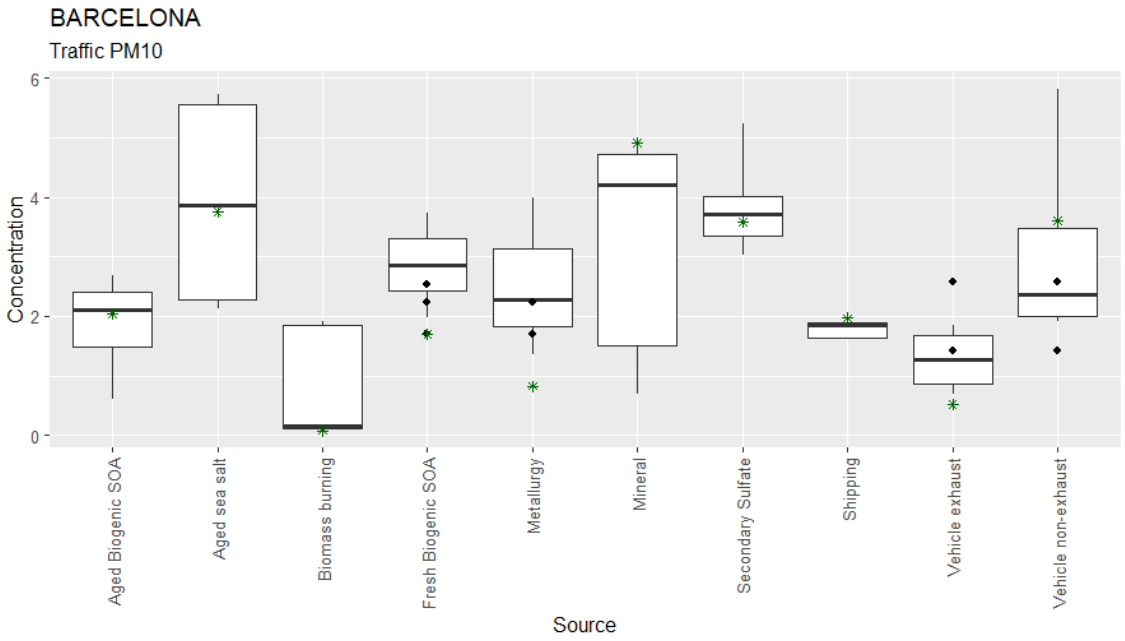

Figure 5. *Uncertainty intervals of PMF source contributions (µg/m³) in Barcelona traffic PM_{10} due to the exclusion of different families of analytes. The case(s) in which a factor is not identified is not presented (i.e. null contribution). Stars indicate the base reference solution. Dots indicate fusions of factors. Adopted from Amato et al. (2024).*

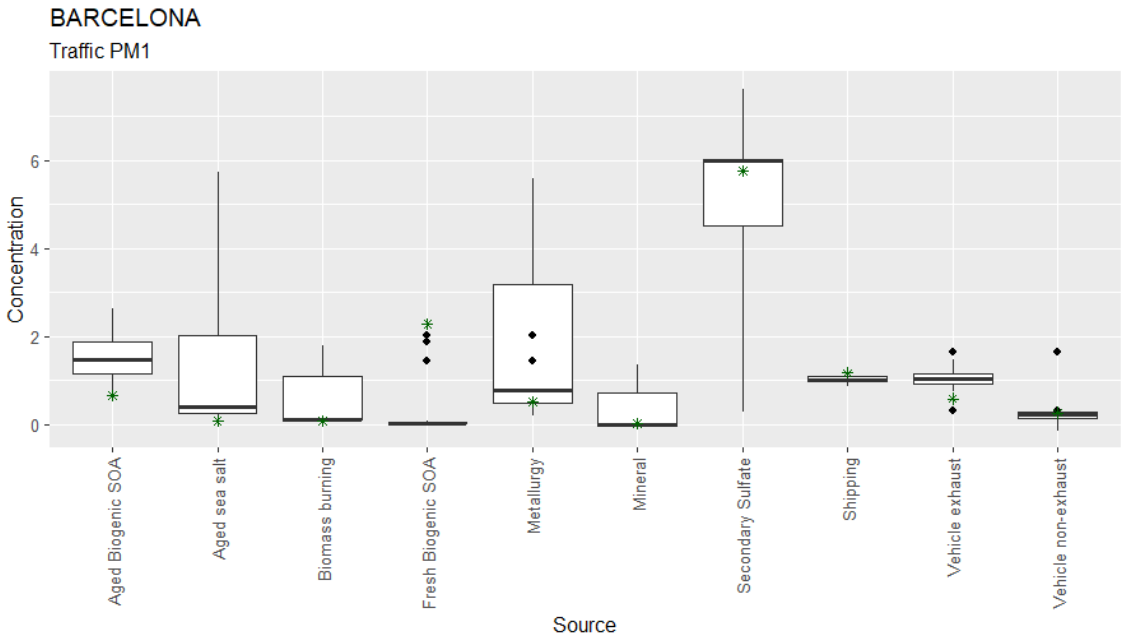

***Figure 6**. Uncertainty intervals of PMF source contributions (µg/m^3) in Barcelona traffic PM_1 due to the exclusion of different families of analytes. The case(s) in which a factor is not identified is not presented (i.e. null contribution). Stars indicate the base reference solution. Dots indicate fusions of factors. Adopted from Amato et al. (2024).*

Shipping: The shipping emissions were identified only in Barcelona due to the presence of the harbour and traced by V and Ni. As expected, such contribution was missing when elements were excluded from the PMF analysis. Among the rest of solutions, the uncertainty due to the different input components selection was narrow and estimated in 8% in PM_{10} and 12% in PM_1 with a generic underestimation of 6–20% in source contributions.

Industrial sources: Industrial factors were identified only in Milan and Barcelona and traced by Pb, Ni, Br, Zn and Mn in Milan, and Pb, Zn, Mn, Cd and As in Barcelona. This factor has been identified in Grenoble in some other PMF studies (Weber, 2019; Borlaza et al., 2021), but even then, only represented a few % of the PM. While in Milan this industrial factor was sensitive only to the presence of elements, in Barcelona, it was also merged to the fresh biogenic SOA (cis-pinonic acid from a-pinene oxidation) in several cases, when excluding ions, non-polar organics, or ammonium. This merging is interpreted as transport related as both Industries and forests are located to the NW sector of the monitoring city site (Amato et al., 2016). In those cases, however, the total source contributions were much smaller than the sum of industrial and fresh biogenic SOA contribution of the base solution. The uncertainty due to the selections of input components was quite narrow in Milan (40%), but very large in Barcelona (overestimated up to a factor of 5). The reason of such difference is unclear.

Secondary organic aerosols: In Grenoble, the base solution provided two factors related to SOA: Aged Biogenic SOA and Anthropogenic SOA. Both of them were sensitive to their tracers, namely the oxidation products of isoprene (α-methylglyceric acid (α-MGA) and 2-methylerythritol (2-MT)) and of α-pinene (hydroxyglutaric acid (3-HGA)) (Carlton et al., 2009; Jaoui et al., 2008) for biogenic SOA and acenaphthenequinone, 6H–dibenzo[b,d]pyran-6-one, 1,8- naphthalic anhydride and 2,3-dihydroxy-4-oxopentanoic acid (DHOPA) for anthropogenic SOA. In Barcelona, the same was true for the Aged Biogenic SOA factor, traced by malic acid, 3-hydroxyglutaric acid, methylbutanetricarboxylic acid (3-MBTCA), 2-methylglyceric acid, 2-methylthreitol, 2-methylerythritol, and fresh Bio SOA traced by cis-pinonic acid. In Milan, no SOA factor was identified due to the lack of tracers. The uncertainty due to the different input components selections was very narrow for Aged Biogenic SOA (3%) but very large for Anthropogenic SOA (40% in Grenoble and 120% in Barcelona), resulting in a systematic overestimation (except at

the Traffic site for PM_{10} in Barcelona) of Anthropogenic SOA due mostly to one large peak, where concentrations can vary up more than 100%.

Secondary inorganic aerosols: In Grenoble, a single SIA factor was identified in the base case solution. The reason was unclear, since other PMF works at this site have generally indicated clear separation of sulfate-rich and nitrate-rich factors (Weber et al., 2019; Borlaza et al., 2021). Such SIA factor was identified as long as ions were selected as input information. If GC/EI-MS analytes were excluded, the SIA factor was split in two the factors of Nitrate-rich and Sulfate-rich, but source contributions were largely overestimated compared to the base case. In Barcelona, a single SIA factor was also identified, although more related to sulfate than nitrate, probably due to the dominance of warmer months in the sampling campaigns. Such Sulfate factor was always identified since it could be traced either by S or SO_4^{2-}. In Milan, secondary sulfate factor and secondary nitrate factor were separated in all solutions except when ions were not used as input species. In that case, Secondary Sulfate (traced by S) contributions were increased by approximately 50%, probably due to the higher ammonium content. Among the rest of the solutions, the uncertainty due to the different input components selection was a general overestimation.

Dust sources: In all cities, the mineral factor was found in the base case and characterized by the enrichment in Al, Si, Ca, Ti, Rb, Li, Rb and Sr. Consequently, it was sensitive to the presence of these elements among the input species. Among the rest of the solutions, the uncertainty due to the different input components selection was estimated at ±11% in Milan and ±13% in Grenoble, but large in Barcelona (±39%) with a systematic underestimation.

Sea salt: The identification of the sea salt factor was more site-dependent due to several reasons. In Barcelona, it was traced either by ions (Cl^-, NO_3^-, Mg^{2+}) or elements (Na, Cl, Mg, S) so that it was always found, and even split in two factors (aged and fresh) when OC/EC or polar organics were not selected as input species. In Grenoble, no elemental Na nor Cl were available so that the identification of sea salt was sensitive to the ions analysis. In Milan, the sea salt was merged to road salt contributions, and it was sensitive to the elemental analysis. Among the rest of solutions, the uncertainty due to the different input components selection was estimated in 33–45% among the three cities, generally symmetric with respect to the reference value.

Primary biogenic particles: Two factors related to primary biogenic aerosols were identified in Grenoble thanks to the analysis of specific tracers of Fungal spores (arabitol and sorbitol; Bauer et al., 2008; Caseiro et al., 2009; Rogge et al., 2007; Yttri et al., 2011) and plant debris (odd number higher alkanes (C27 to C31; Rogge et al., 1993). As expected, both factors were sensitive to the presence of their specific tracers, but, in addition, we observed a merging of Fungal spores' factor with the Primary traffic factor, when elements were excluded from the analysis. The reason of that remained unclear. Among the rest of the solutions, the symmetric uncertainty due to the different input component selection was estimated in 23% and 18% respectively.

Table 2. *The different PMF solutions in Grenoble varying the number of families of components.*

Grenoble	Characterized mass (%)	Reconstructed mass (%)	# of factors	Type of factors (% of contribution)
Base solution	67	93	9	Mineral (17%) Sea salt (4%) Primary Traffic (9%) Anthropogenic SOA (3%) Biogenic SOA (13%) Plant debris (11%) Fungal spores (4%) SIA (17%) Biomass burning (18%)
Excluding EC/OC	37	93	9	Mineral (16%) Sea salt (4%) Primary Traffic (8%) Anthropogenic SOA (2%) Biogenic SOA (13%) Plant debris (10%) Fungal spores (5%) SIA (15%) Biomass burning (19%)
Excluding	41	90	7	Mineral (19%)

ions				Primary Traffic (10%) Anthropogenic SOA (5%) Biogenic SOA (14%) Plant Debris (12%) Fungal spores (4%) Biomass burning (26%)
Excluding elements	62	91	7	Sea salt (5%) Primary Traffic + Fungal spores (13%) Anthropogenic SOA (4%) Biogenic SOA (14%) Plant Debris (15%) SIA (20%) Biomass burning (20%)
Excluding GC/EI-MS analytes	67	92	8	Mineral (13%) Sea salt (2%) Primary Traffic (5%) Nitrate (16%) Anthropogenic SOA (2%) Fungal spores (7%) Sulfate (26%) Biomass burning (20%)
Excluding PAHs	67	92	8	Mineral (15%) Sea salt (2%) Primary Traffic (13%) Biogenic SOA (14%) Plant Debris (11%) Fungal spores (5%) SIA (19%) Biomass burning (13%)
Excluding Levoglucosan, arabitol, sorbitol	65	93	8	Mineral (19%) Sea salt (5%) Primary Traffic (10%) Anthropogenic SOA (3%) Biogenic SOA (13%) Plant Debris (9%) SIA (14%) Biomass burning (20%)
Excluding HULIS	64	93	9	Mineral (17%) Sea salt (4%) Primary Traffic (9%) Anthropogenic SOA (3%) Biogenic SOA (13%) Plant Debris (10%) Fungal spores (4%) SIA (14%) Biomass burning (18%)

Table 3. *The different PMF solutions in Barcelona varying the number of families of components.*

Barcelona	**Characterized mass (%)**	**Reconstructed mass (%)**	**# of factors**	**Type of factors (% of contribution)**
Base solution	47	94	10	Aged biogenic SOA (6%) Vehicle exhaust (7%) Biomass burning (1%) Mineral (13%) Shipping (9%) Fresh biogenic SOA (9%) Aged sea salt (11%) Metallurgy (3%) Vehicle non-exhaust (12%) Regional Sulfate (21%)
Excluding EC/OC	31	94	10	Aged biogenic SOA (11%) Vehicle exhaust (3%) Biomass burning (6%) Vehicle non-exhaust (10%) Mineral (12%) Shipping (8%) Fresh biogenic SOA + Metallurgy (6%) Aged sea salt (10%) Fresh sea salt (7%) Regional Sulfate (22%)
Excluding ions	39	94	8	Aged biogenic SOA (9%) Vehicle exhaust (9%) Biomass burning (7%) Mineral (11%) Shipping (9%) Fresh biogenic SOA + Metallurgy (5%) Aged sea salt (14%) Vehicle non-exhaust (9%) Regional Sulfate (21%)
Excluding elements	36	91	6	Aged biogenic SOA (7%) Traffic (8%) Biomass burning (11%) Fresh biogenic SOA + Fresh sea salt (9%) Secondary nitrate (31%) Regional Sulfate (24%)
Excluding	47	94	9	Vehicle exhaust (11%) Vehicle non-exhaust (6%)

polar organics				Hopanes (1%) Mineral (13%) Shipping (7%) Metallurgy (5%) Aged sea salt (16%) Fresh sea salt (7%) Regional Sulfate (28%)
Excluding NH_4^+	45	94	10	Aged biogenic SOA (13%) Vehicle exhaust (8 %) Vehicle non-exhaust (8 %) Biomass burning (2%) Mineral (11%) Shipping (8%) Fresh biogenic SOA + Metallurgy (6%) Aged sea salt (14%) Fresh sea salt (5%) Regional Sulfate (19%)
Excluding non-polar organics	47	94	9	Aged biogenic SOA (11%) Traffic (10%) Biomass burning (1%) Mineral (13%) Shipping (7%) Fresh biogenic SOA + Metallurgy (9%) Aged sea salt (14%) Fresh sea salt (5%) Regional Sulfate (23%)

Table 4. *The different PMF solutions in Milan varying the number of families of components.*

Milan	**Characterized mass (%)**	**Reconstructed mass (%)**	**# of factors**	**Type of factors (% of contribution)**
Base solution	69	99	8	Vehicle exhaust (9%) Vehicle non-exhaust (14%) Secondary sulfate (23%) Secondary nitrate (18%) Mineral (15%) Biomass burning (8%) Industrial (8%) Sea/road salt (4%)
Excluding EC/OC	42	99	8	Vehicle exhaust (9%) Vehicle non-exhaust (14%) Secondary sulfate (22%) Secondary nitrate (18%) Mineral (16%) Biomass burning (9%) Industrial (7%) Sea/road salt (4%)
Excluding ions	39	96	7	Vehicle exhaust (10%) Vehicle non-exhaust (19%) Secondary sulfate (31%) Mineral (13%) Biomass burning (13%) Industrial (4%) Sea/road salt (6%)
Excluding elements	57	98	4	Traffic (43%) Secondary sulfate (30%) Secondary nitrate (19%) Biomass burning (7%)
Excluding sugars	68	99	7	Vehicle exhaust (8%) Vehicle non-exhaust (18%) Secondary sulfate (23%) Secondary nitrate (20%) Mineral (13%) Industrial (10%) Sea/road salt (7%)

2.4 Discussion of the results

The results of the sensibility analyses show that road traffic sources are generally identified by analysing at least two groups of analytes, namely EC/OC and PAHs and/or elements. The exhaust source resulted to be less sensitive to the choice of analytes, although source contributions estimates could deviate significantly up to 44% (positively or negatively).

To identify and to apportion the non-exhaust PM contribution, it is clearly necessary to analyse specific elements (Cu, Sn, Sb, Ba, Zn, Fe). Still, the exclusion of another group of analytes can provoke a bias of non-exhaust contributions up to 50%.

The choice of not analysing non-polar organics likely caused the loss of separation of exhaust and non-exhaust factors, thus obtaining a unique road traffic source, which provoked a significant bias of total contribution.

Levoglucosan was in most cases crucial to identify biomass burning contributions in Milan and in Barcelona, in spite of the presence of PAHs in Barcelona, while for the case of Grenoble, even discarding levoglucosan, the presence of PAHs allowed identifying the BB factor. Modifying the rest of the analytes provoked a systematic underestimation of biomass burning source contributions.

SIA factors resulted to be generally overestimated with respect to the base case analysis, also in the case that ions were not included in the PMF analysis.

Trace elements were crucial to identify shipping emissions (V and Ni) and industrial sources (Pb, Ni, Br, Zn, Mn, Cd and As). When changing the rest of the input variables, the uncertainty was narrow for shipping but large for industrial processes. Major and trace elements were also crucial to identify the mineral/soil factor at all cities. The modelling error when other analytes were excluded was estimated to be very narrow in Milan and Grenoble (11–13%) but large in Barcelona (39%) with a systematic underestimation.

Biogenic SOA and Anthropogenic SOA factors were sensitive to the presence of their molecular tracers, being OC alone unable to separate a SOA factor. This is contrarily to what has been found by Veld et al. (2022) where a SOA-like factor was found when combining urban and rural sites in a single PMF matrix. In addition, while Biogenic SOA contributions were very robust in the sensitivity analysis, the opposite was found for the Anthropogenic SOA.

Sea salt was traced either by ions (Cl^-, NO_3^-, Mg^{2+}) or elements (Na, Cl, Mg, S) so that it was generally well identified, and even splitted in two factors (aged and fresh) depending on the input matrix. Error interval ranged within 33–45%.

Arabitol and sorbitol were crucial to detect fungal spores while odd number higher alkanes (C27 to C31) were critical to detect plant debris. When other groups of analytes were excluded the error intervals in source contributions were symmetric and estimated in 23% and 18%, respectively.

2.5 Recommendations for off-line source apportionment based on 24h resolution PM chemistry data

Based on the above results, the following general recommendations can be drawn for selecting the most appropriate species as input for PMF receptor modelling:

- For doing source apportionment analysis of PM, use PMF US-EPA version 5 (https://www.epa.gov/air-research/positive-matrix-factorization-model-environmental-data-analyses).
- In order to optimize the PMF analysis and evaluate its performance use these two guides:
  - European Guide on Air Pollution Source Apportionment with Receptor Models (https://publications.jrc.ec.europa.eu/repository/handle/JRC117306)
  - CEN/TS 17458:2020. Ambient Air - Methodology to Assess the Performance of Receptor Oriented Source Apportionment Modelling Applications for Particulate Matter.
- In order to perform an adequate SA analysis with the PMF receptor modelling technique, a database including at least EC/OC, major ions (using ion chromatography), major and trace elements (by ICP-AES and/or ICP-MS), and analysis of biomass burning tracers (either by LC-PAD or by GC-MS) should be mandatory. This allows to identify most of the main contributors to PM in Europe, i.e., dust, sea-salt (eventually separated into fresh and aged sea salt), traffic emissions (eventually separated between exhaust and non-exhaust), biomass burning aerosols, industrial emissions (possibly separated in different types depending on the knowledge of the emissions at the site), and possibly shipping emissions (characterized with V and Ni). It also leads to the determination of secondary inorganic aerosol factors (commonly separated into SO_4^{2-} and NO_3^- rich components.

However, such an approach does not allow to properly apportion primary biogenic emission, nor the various SOA fractions.

- If IC measurements include MSA and oxalate, it may lead to further determination of the main marine SOA fraction (traced with MSA) and to roughly apportion aged SOA factors originating from various origins (traced with oxalate),
- HPLC-PAD measurements for sugar alcohols (in particular arabitol and mannitol) may lead to further determination of primary biogenic aerosol that can be a substantial PM fraction at some sampling sites, especially from spring to late autumn.

A refined PMF analysis, including the determination of further sources, requires additional measurements, such as secondary biogenic emission, including tracers such as 3-MBTCA and 2-MT, measured with techniques like GC-MS, LC-MS, and/or IC-MS.

Inclusion of a range of PAH measurements (or some PAH derivatives) may lead to some improvement in some combustion source separations but results should be studied with caution in terms of chemical profile since these species are coming from many various origins.

Inclusion of species like higher alkanes may also lead to some improvements in organic sources determination, especially plant debris, but results should be considered with caution.

3. SOURCE APPORTIONMENT BASED ON HIGH-TIME RESOLUTION ORGANIC AEROSOL MEASUREMENTS

3.1. Methodology

Non-refractory PM_1 (NR-PM_1) is a group of pollutants, defined by their capacity to flash-vaporise at 600º, which are the main contributors to fine aerosol in Europe (Bressi et al., 2021). Near-real-time measurements of NR-PM_1 species are usually carried out with the aerosol chemical speciation monitor (ACSM) (in two versions depending on its mass spectrometer, quadrupole (Q-ACSM) or time-of-flight (ToF-ACSM)) or the aerosol mass spectrometer (AMS). These instruments use a mass spectrometer to measure the spectral composition of the incoming air after vaporisation and ionisation. Posteriorly, the ions are deconvolved to NR-PM_1 compounds using a fragmentation table and electronic signals to mass through calculations needing routine calibrations. After these steps, the software provides the non-refractory time series of OA, SO_4^{2-}, NO_3^-, NH_4^+, and Cl^-. The OA information can also be exported as a matrix of all the spectral species and time series. An error matrix is also provided and calculated as in Ulbrich et al. (2009). More information on the operation of the ACSMs can be found in the PM speciation guidance document (Service Tool ST3) of the RI-URBANS.

The most widely used and further developed receptor model for OA SA purposes is the Positive Matrix Factorisation (PMF) using the multi-linear engine 2 (ME-2, Paatero et al., 2009). This model provides OA sources that explain the introduced matrices as a linear combination plus an error matrix, which is minimised iteratively. These sources comprise a time series, showing the temporal evolution of the source and the profile, and the proportions of the ions that contribute to that source. The profiles are considered static by the algorithm throughout the whole period of analysis, an assumption that has been refuted since the sources' fingerprints are expected to vary along the seasons (Canonaco et al., 2015), especially for the longer ACSM sampling deployments.

In this context, Chen et al. (2022) developed a harmonized procedure for OA source apportionment based on long-term measurements using aerosol mass spectrometry. It consists, broadly speaking, of a two-step process: the first one entailing the so-called *seasonal* PMF and the second one the *rolling* PMF. Firstly, the OA matrices are split seasonally and PMF is conducted separately for each. This is called *seasonal* PMF since it can characterize the seasonal evolution of PMF profiles. In this first phase, the PMF runner determines the potential sources for each

season and tests the stability of these sources. The application of constraints to guide the model with a priori knowledge of the site sources is recommendable in this phase, as well as the evaluation of the obtained factors with collocated measurements. This phase outputs consist of bootstrapped seasonal profiles and time series.

The second phase entails applying the *rolling* PMF to the whole dataset. Rolling PMF applies PMF in user-defined windows (usually 14 days but could also be 7 or 28 days) with one-day shifts providing time-evolving profiles. This step implies constraining the primary profiles with reference profiles or, preferably, the outcoming seasonal bootstrap profiles with many repeats for each PMF window. After running PMF, the selection of the most coherent runs is based on several user-defined criteria usually using correlation with, e.g., external source tracers, known ratios between OA markers, and evaluation of source diel/weekly/monthly cycles. Once the non-optimal runs are filtered out, the remnants are averaged and bootstrapped to obtain the final PMF solution. The rolling PMF should not be applied directly since the seasonal testing phase reveals crucial information about seasonal variabilities. Alternatively, rolling PMF is demonstrated to provide more accurate results than seasonal (Via et al., 2023), which justifies the latter phase of SA.

In the next section, we present a European overview of SA results of 19 urban/suburban/traffic sites plus one background site to use as a reference (Hoppenheissenberg). The following section tackles the methodology for such data compilation, the overview results, and some recommendations on the OA SA.

3.2. Pan-European overview of source apportionment

3.2.1 Methodology

The SA of online OA presented here has been performed by each site user. PMF matrices can be obtained by the usual data treatment software (acsm_local_1.6.1.1) from Aerodyne Inc. (Billerica, US) and Tofware (Tofwerk AG, Thun, Switzerland), both written in Igor Pro (Wavemetrics inc., Lake Oswego, Oregon, USA). In all cases, the step function for uncertainties downweighting (Paatero and Hopke, 2003) was applied, which consists of a moderate and high increase of the uncertainties of all those species which present weak and bad signal-to-noise ratios, respectively. The participating sites details, use of rolling or seasonal methodologies, the anchored factors, the bootstrap application, and the paper where SA results have been published are listed in Table 5. The location and the type of each site are depicted in Figure 6. The standard protocol for SA is published by Chen et al. (2022), although some sites might have justified deviations shown in the aforementioned table. PMF has in all cases been conducted through the Source Finder software SoFi Pro (Datalystica Ltd., Villigen, Switzerland) as described in Canonaco et al. (2021). More specific information on the SA details can be found in the published scientific articles cited therein.

Table 5. *Source apportionment methodology details about the 18 available sites' results including the PMF method employed, the profiles anchored with a priori information, the bootstrap application, and the published results reference. CDCE stands for Composition-Dependent Collection Efficiency, R stands for Rolling, S stands for Seasonal.*

Site	Acronym	Type	Instrument	PMF method	Reference profiles	Boot strap	Published results
ATOLL, Lille, FR	ATOLL	SU	Q-ACSM	R	HOA, BB	Y	Chebaicheb et al. 2023
Palau Reial, Barcelona, ES	BCN	UB	Q-ACSM	R	HOA, COA, BBOA	Y	Via et al. 2021
Bologna, IT	BO	UB	AMS	S	HOA, COA, BBOA	N	Paglione et al. 2020
CAO, Nicosia, CY	CAO-NIC	UB	Q-ACSM	S	HOA, BBOA	N	Christodolou et al. 2023
Demokritos, Athens, GR	DEM	UB	ToF-ACSM	R, S	HOA, COA, BBOA	Y	Zografou et al. 2022
Dublin, IE	DUB	UB	Q-ACSM	R	HOA, Peat, Coal, Wood	Y	Lin et al. 2021
Granada, ES	GRA	UB	Q-ACSM	S	HOA, BBOA	N	-
Hohenpeissenberg, GE	HPB	RB	Q-ACSM	S	-	N	-
INOE, Bucharest, RO	INO	SU	Q-ACSM	R	HOA, BBOA	Y	Mărmureanu et al. (2020)
Krakow, PO	KRK	SU	Q-ACSM	R	HOA, BBOA, CCOA	Y	Tobler et al. 2021
Marylebone road, London	LON-MR	TR	Q-ACSM	R	HOA, COA, BBOA	Y	Chen et al. in prep.
N-Kensington, London, UK	LON-NK	UB	Q-ACSM	R	HOA, COA, BBOA	Y	Chen et al. in prep.
Longchamp, Marseille, FR	MAR-LCP	UB	ToF-ACSM	R	HOA, COA, ShIndOA	Y	Chazeau et al. 2022

Milano, IT	MI	UB	AMS	S	COA	N	-
Padova, IT	PD	UB	AMS	S	HOA,	N	-
SIRTA, Paris, FR	SIRTA	SU	Q-ACSM	S	HOA, BBOA	Y	Zhang et al. 2019
Tartu, EE	TAR	UB	Q-ACSM	R	HOA, COA, BBOA	Y	Chen et al. 2022
Vilnius, LT	VLN	UB	Q-ACSM	S	LOA, POA, BBOA	N	Pauraite et al. 2022
Zurich, CH	ZUR	UB	Q-ACSM	R	HOA, COA, BBOA, CSOA	Y	Chen et al. 2022

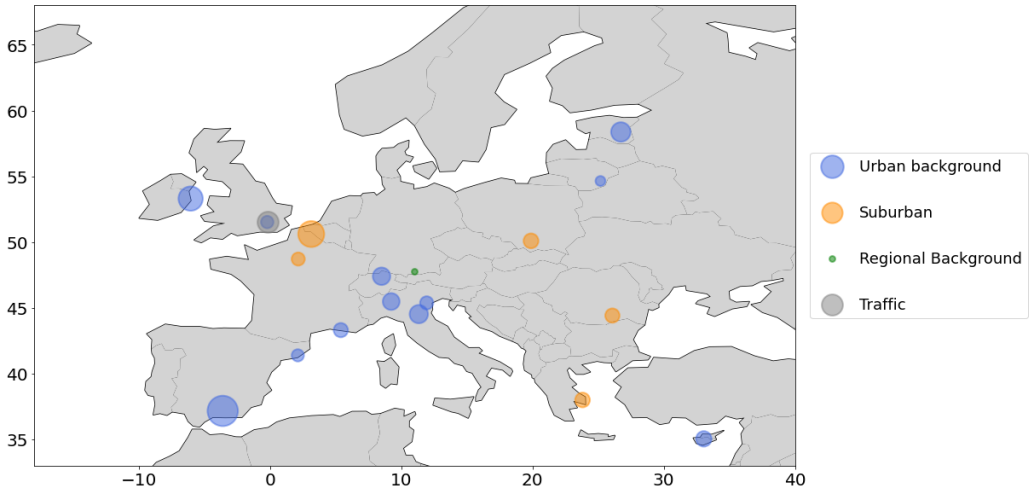

Figure 6. *European spatial distribution of the NR-PM$_1$ concentrations at urban sites compiled. The size of the circles corresponds to mass concentration.*

3.2.2 Pan-European overview of results

The main OA sources of the sites participating in this overview are shown in Figure 7. Organic aerosol sources can be divided into primary and secondary. Primary sources include hydrocarbon like OA (HOA, and also HOA1, HOA2), biomass burning OA (BBOA), cooking-like OA (COA), amine OA (amine-OA), wood, coal, and peat OA, coal combustion OA (Coal OA), shipping + industry OA (ShINDOA), local OA (LOA); primary OA (POA); and cigarette-smoke OA (CSOA). Amongst secondary OA there are less-oxidised oxygenated OA (LO-OOA), more-oxidised oxygenated OA (MO-OOA), and generic oxygenated OA (OOA). Also, there are different mixings of OOA+BB (OOA_BB, OOA_BBaq).

The proportion of SOA amongst all the sites was 41–92%, with a mean and standard deviation of 65% and 13%, respectively. As it can be seen in Figure 6 the regional background site, Hopenheissenberg, was the one with the lowest proportion of primaries, as expected from remote background sites. Contrarily, the urban background sites presented the minimum SOA/OA ratios, even though there is a high variability of sources amongst sites.

Even though this was not directly comparable since they do not account for the same time periods, still there were some solid differences in POA sources' proportions which are worth referring to and shown in Figure 7. There were a few sites whose BBOA was the dominant POA source (ATOLL, BO, DUB, INO, MAR-LCP, MI, PD, TAR, and VLN). All the Po-valley sites were POA-BBOA-dominated. Conversely, although traffic was not the main primary source at almost any site (only at CAO-NIC, GRA), it was present at every site, even in the remote background ones, implying that traffic was not only a local source but also an OA source of regional influence. In addition, COA was also a relevant source, especially in urban background sites (BCN, BO, DEM, LON-NK, MAR-LCP, MI, ZUR) and in the traffic site (LON-MR), but it was not detected at suburban sites. This implied that this source was unstable under transport conditions from the most densely populated areas to city outskirts. Coal combustion was a relevant source only in Dublin and Krakow, although in the latter it was the most prominent primary source. Other primary sources present in this study in minor proportions were amine-OA, wood and peat burning, Shipping + Industry OA, local OA, a generic primary OA source, and cigarette smoke OA.

Regarding secondary OA, all sites achieved the differentiation of two main SOA factors differentiated upon their degree of oxidation into Less Oxidised-OOA and More Oxidised-OOA, except for the Granada and Padova sites, probably because of the campaigns being short and in winter. In summer, according to various SA studies, the OOA is easy to differentiate, with the formation of LO-OOA due to the enhancement of photochemical reactions and of MO-OOA which denotes a more aged and regional origin (Canonaco et al., 2014; Via et al., 2021). In Zurich, both OOA and LO-OOA/MO-OOA pair were present because both SOA factors were differentiated in the warmer periods but not in the colder seasons. The Bologna site also achieved the differentiation of two more OOAs related to BBOA emissions giving the capacity of the AMS to resolve individual species.

The LO-OOA-to-MO-OOA ratio has been used in many studies to assess the secondary aerosol ageing (Zhan, 2021; Duan, 2020). This quantity was in most sites below one meaning the aged SOA (MO-OOA) proportion was higher than the fresh SOA (LO-OOA), with the minimum value found at INO (ratio of 0.43). However, at the remote background site, this ratio was higher than 1, entailing that the aerosol was fresher in this remote site, probably due to proximity to bio-SOA enhancement in a more natural area. Also, Milano-Pascal and Vilnius sites presented a LO-OOA-to-MO-OOA ratio above 1, indicating a potential source of fresh aerosol nearby or little recirculation of aged aerosol.

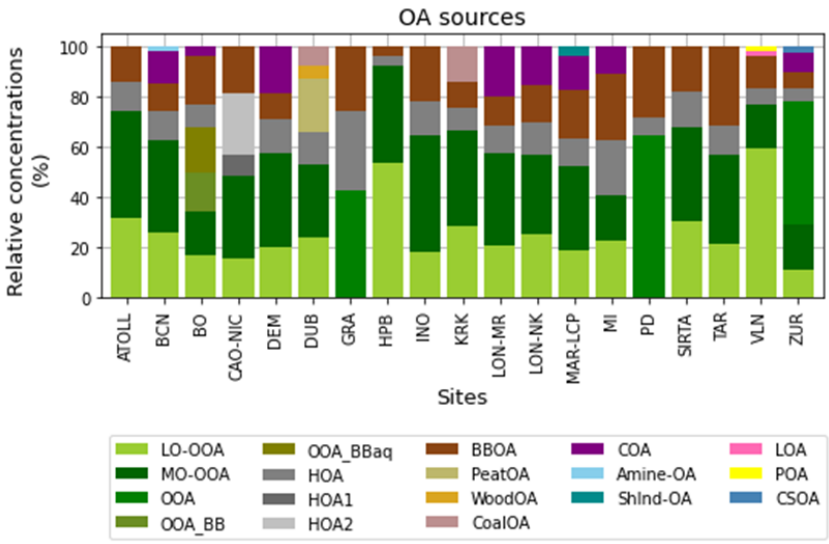

Figure 7. *Relative mean site OA composition of all sites providing source apportionment results.*

Figure 8 shows the compound-normalised diel cycles of OA sources at each site. Here we describe the main sources of diel cycles in a point-by-point manner:

- LO-OOA: The fresher secondary OA behaved differently amongst sites. Some sites (BO, DUB, HPB, KRK) presented a concentration increase around midday probably related to the photochemical reactions' enhancement due to higher solar irradiation at noon. Also, there were some sites (BCN, CAO-NIC, DEM, LON-MR, MAR-LCP, TAR, ZUR) in which the maximum concentrations happened during 3–6 AM, probably due to night-time chemistry SOA pathways and a strong dilution effect of these particles around midday due to a wider boundary layer. As a conclusion, LO-OOA diel cycles depended strongly on the local meteorology and available SOA precursors, which led to differentiated SOA generation pathways.
- MO-OOA: Diel cycles of aged SOA were more clearly marked than those of LO-OOA, since they were less dependent on precursor availability and their amounts were more related to regional air circulations. This was seen at most sites, in which the concentrations increase around noon even if the dilution factor was higher due to a higher boundary layer height. This can be explained due to a higher fresh-to-old SOA conversion rate at noon related to higher irradiation, and/or to breeze-advected air masses transporting aged aerosol.

- HOA: The temporal trend is mainly bimodal, with a peak around 7–8 AM and around 6–7 PM, especially in urban sites related to road traffic intensity peaks in cities. Around noon, the concentrations presented a clear decrease likely due to a decrease of road traffic activities and an increase of the boundary layer height favouring aerosol dilution. This pattern was subtler in suburban sites (INO, ATOLL, KRK, SIRTA) and non-existing in HPB, due to the higher distance to the pollutant source and transportation of these pollutants through urban-to-suburban advections.

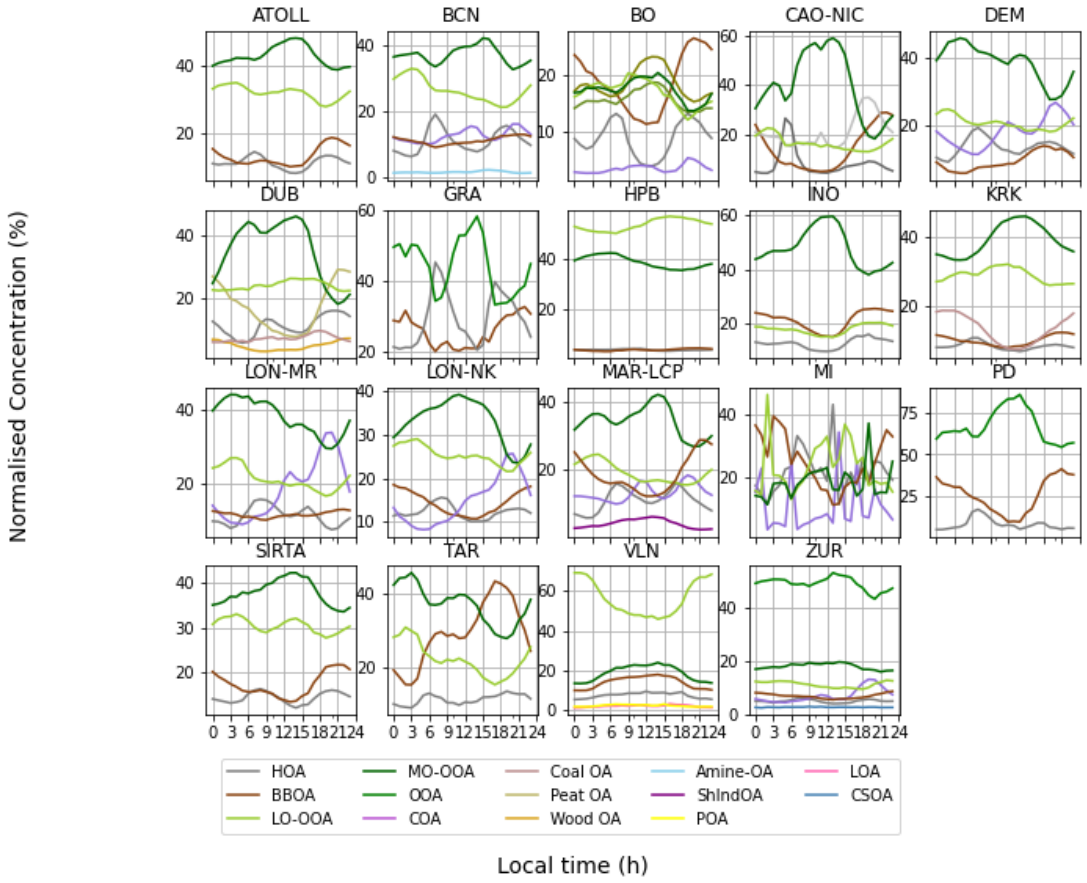

Figure 8. *Normalised diel cycles of OA sources for each site. Time presented in these plots is UTC.*

- BBOA: The diel trend of this factor was rather consistent and presented the maximum or quite high concentrations during evening hours (6–10 PM) at all sites. This was likely related to solid fuel burning for residential heating at the late hours of the day. Also, at some sites it also presented a wide minimum around noon due to the increase of the boundary layer. While this factor reflected primary emissions, solid fuel burning emissions may have also contributed to secondary OA in the OOA fractions (Chebaicheb et al., 2023).
- COA-like: Found in BCN, BO, DEM, LON-MR, LON-NK, MAR-LCP, MI, and ZUR, this source presented a homogeneous diel pattern displaying two characteristic peaks related to cooking hours, the first around noon (11–1 AM) and another one at evenings (6–8 PM). Some sites also presented a clear peak during morning traffic rush hours (6–8 AM) due to a likely entanglement of this factor with traffic emissions.
- Other sources:
  - Coal OA: Clear increase during nights due to the use of coal for residential heating and decrease in the central hours of the day due to higher dilution conditions.
  - Wood OA: Smooth double peaks at 9–11 AM and 6–8 AM (Li et al., 2021).
  - Peat OA: Soft decrease around noon, likely linked to residential heating (Li et al., 2021).
  - ShIndOA: Increasing around noon, related to breeze advections transporting from the shipping and industry area (Chazeau et al., 2022).

- Amine-OA: Rather flat, small increase during evenings with the land-breeze transport from industrialised areas (Via et al., 2023).
- CSOA: Rather flat, no clear diel cycle.
- POA: Increase around noon, probably due to breeze advection.

Regarding intra-year cycles, monthly plots are shown in Figure 9, although for those sites whose datasets consist of short campaigns, these year cycles are incomplete.

Regarding POA factors, COA presented a less marked trend, probably because of an equal emission pattern throughout the year. A very consistent trend amongst sites was that of BBOA, which presented a clear minimum in warm months and maximum concentrations in December, January and February. The annual cycle of traffic source (HOA) was also at minimum in the summer and at maximum in the winter due to higher frequency of stagnation episodes in the cold months. SOA factors (LO-OOA and MO-OOA) both presented higher concentrations in the summer likely due to the higher photochemical activity in that season. Whilst the MO-OOA annual evolution is flatter, likely indicating that this is a transported and permanent pollutant, the LO-OOA peak in summer is narrower, indicating a more local behaviour.

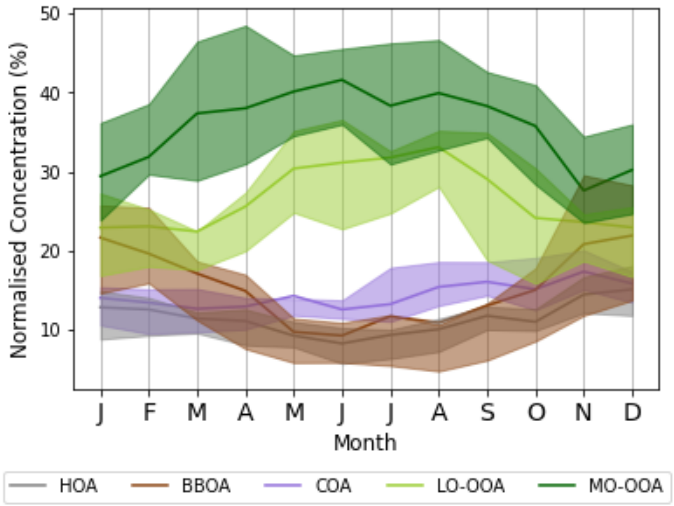

Figure 9. *Monthly cycles of OA sources of all sites included in this overview. Percentiles 25 and 75 are shown in shaded areas and the mean in solid lines.*

3.3 Recommendations for offline source apportionment based on organic aerosol measurements of high time resolution

This section provides the current state-of-the-art recommendations for SA of OA long-term timeseries based on the protocol proposed by Chen et al. (2022) along with some more methodological insights obtained posteriorly which update and complement such protocol.

- Source apportionment of OA through PMF is recommended for extracting organic PM sources. Following the aforementioned protocol is advised for generating robust and accurate results that can be comparable with a large community of PMF users.
- This protocol enforces the application of PMF through two complementary methodologies, seasonal and rolling PMF. The seasonal PMF consists in splitting the initial matrices by seasons, applying PMF independently to all of them and after that, concatenating the resulting time series and showing the seasonal profiles. Rolling PMF was developed so that a rolling PMF window of 7–28 days (user preference may be used) sweeps the whole period and hence it adapts better profile-wise. This method was shown to enhance the PMF performance (Via et al., 2022), although some prior testing with seasonal PMF is advised before applying rolling PMF. However,

the current protocol highlights the use of seasonal PMF to inspect the OA sources seasonally and a posterior rolling PMF use for definitive profile-evolving profiles.

- Another extended practice is the user of constraints to guide the model towards the a priori knowledge of sources at the site. For such purpose, the a-value approach is recommended to anchor a reference profile or time series with *a* being the degree of freedom given to the model to mimic the anchor. This procedure is further explained in Chen et al. (2022). In Via et al. (2022), it can be seen that the impact of the choice of reference profiles is remarkable, hence local profiles from the site are further recommended.
- Bootstrapping PMF solutions is also highly advised in both seasonal and rolling phases since it provides statistical rotational ambiguity error assessment.
- However, other receptor models can be advisable for SA purposes depending on the aim of the study. For instance, the chemical balance model (CMB; Watson et al., 1991), which uses known profiles of the factors and only the time series are adjusted, could be advisable for datasets of known underlying OA sources profiles. Also, a recent study has proven that the Bayesian Autocorrelated Matrix Factorisation provides even more accurate results with comparison to PMF (Rusanen et al., 2024), but it is yet to be tested in real-world datasets.
- Moreover, the acquisition of parallel measurements is also advised for monitoring purposes of co-variating species with sources. If clearly correlated, these ancillary measurements can even be used as an anchor for PMF time series anchoring. Besides for that purpose, the most advised co-located measurements are black carbon, if possible speciated upon their origin into liquid and solid fuel, used both for PM_1 mass closure and for verifying the correlation with traffic and biomass burning sources. Other useful ancillary measurements are NO, NO_2, SO_2, CO and O_3 gases concentrations and metals at high-time resolution.

4. SOURCE APPORTIONMENT BASED ON HIGH TIME RESOLUTION TRACE ELEMENTS MEASUREMENTS

4.1 Methodology

Recent advancements in technology have made it possible to create instruments with integrated analytical capabilities for near-real-time and continuous analysis of atmospheric elements in PM samples (Hasheminassab et al., 2020). One commercially available instrument that offers these features is the Xact 625i Ambient Metals Monitor developed by Cooper Environmental. The Xact allows for automated in situ measurements of elemental concentrations in ambient PM_{10}, $PM_{2.5}$, or PM_1, and users can define a specific set of elements (from 24 to up to 67 elements) to monitor with a sampling time resolution ranging from 15 to 240 minutes (Furger et al., 2017; Tremper et al., 2018). By analysing high-resolution elemental data, it becomes possible to identify sources contributing to episodic or unusual air pollution events.

Until lately, elemental analysis methods typically relied on sample collection, often for 24 hours or more, resulting in good spatial and temporal coverage but low time resolution of the obtained results. One limitation is that some important information such as diurnal patterns or short-term pollution events can be lost or difficult to identify (Manousakas et al., 2021; Viana et al., 2008). In multivariate analysis such as PMF, the quality of the results can be compromised if source emissions exhibit high covariance, as the models rely on the variation between source emissions for source separation. When the time resolution of the elemental composition data is low, it becomes challenging to incorporate enough variation into the dataset with seasonal variation being the primary source of variability.

On the other hand, higher time resolutions (such as 1 hour or less) capture the diurnal variation in source emissions, making it possible to account for short-term events and changes in local meteorology, thereby increasing the overall variation in the dataset.

Since recent years, various studies have utilized the Xact data (Hasheminassab et al., 2020; Liu et al., 2019; Rai et al., 2020a, 2020b, 2021; Wang et al., 2021, 2018; Yu et al., 2019). However, just a few of them (six in total) have presented SA results in Europe (Table 6). Moreover, there is no existing protocol or standard procedure defining the most appropriate methodologies for performing SA on high time resolution elements components available. A synopsis of these SA studies using PMF that took place in Europe is provided in the following section. We also draw some first recommendations for PMF based on these studies in the next section.

4.2 Pan-European overview of source apportionment

The first SA study in Europe using Xact data was the one from Rai et al. (2020). This study used the same data as Furger et al. (2017) for the identification of the sources of the elemental components of PM. Eight different sources were identified in $PM10_{el}$ (elemental PM10) mass driven by the sum of 14 elements (notable elements in brackets): Fireworks-I (K, S, Ba and Cl), Fireworks-II (K), sea salt (Cl), secondary sulfate (S), background dust (Si, Ti), road dust (Ca), non-exhaust traffic-related elements (Fe) and industrial elements (Zn and Pb). The major components were secondary sulfate and non-exhaust traffic-related elements followed by background dust and road dust factors, explaining 21%, 20%, 18% and 16% of the analysed PM_{10} elemental mass, respectively, with the factor mass not corrected for oxygen content. Further, there were minor contributions (on the order of a few percent) of sea salt and industrial sources.

An interesting study has been reported by Belis et al. (2019) consisting of the first published attempt to combine Xact data with that of other high-time resolution instruments. Parallel hourly online measurements were made using the Xact 625 (CES LLC) XRF analyser and the Q-ACSM. The sampling campaign was carried out in January–February 2015 in a background monitoring site located in a small town (Veggiano) near Padua, Italy. To ensure the consistency of the final PMF results, a multistep approach was adopted. In the first step PMF was run with only the offline dataset, in the second step only the online organic data were used and in the third step the PMF run was executed using only the online inorganic species. The sources identified were biomass burning, aged biomass burning, secondary ammonium nitrate and ammonium sulphate, traffic, steel industry and waste thermal treatment.

A study dedicated to assist towards the attribution and quantification of atmospheric nickel concentrations in an industrial area in the UK was published by Font et al. (2022). A campaign measuring metal concentrations in PM_{10} at an hourly resolution was undertaken using the Mobile Atmospheric Research PLatform (MARPL) in Pontardawe (27 November – 24 December, 2015) alongside the long-running UK Heavy Metals monitoring site (Defra). PMF was used to identify the sources and those industrial processes contributing to the ambient concentrations based on the chemical composition. Bivariate polar plots for the factor time series containing Ni in the chemical profile were built and cluster analysis applied to pinpoint and quantify the contribution of each industry to each source process. Two sources were identified to contribute to Ni concentrations: stainless-steel (which contributed to 10% of the Ni burden) and the Ni refinery (contributing 90%). From the stainless-steel process, melting activities were responsible for 66% of the stainless-steel factor contribution.

Another SA study was conducted by Manousakas et al. (2022). This study utilized the longest available size segregated elemental composition dataset until today in Europe. Measurements were performed at an urban background site in Zürich (Zürich-Kaserne), from May 2019 to May 2020. For data collection, they used an ambient metal monitor, Xact 625i, equipped with a sampling inlet alternating between $PM_{2.5}$ and PM_{10}. The use of this switching inlet system allowed to include variables with different size ranges in the dataset, which introduced extra variation and improved the accuracy of estimating emission processes and source fingerprinting. By implementing interpolation and a newly proposed uncertainty estimation methodology, it was possible to obtain and use a combined dataset of $PM_{2.5}$ and PMcoarse (PM_{10}–$PM_{2.5}$) in PMF having data from only one instrument. The combination of the inlet switching system, the instrument's high time resolution, and the use of advanced SA approaches yielded improved SA results in terms of the number of identified sources as the model, additionally to

the diurnal and seasonal variation of the dataset, also utilized the variation from the size segregated data. Thirteen sources of elements were identified, i.e., sea salt (5.4%), biomass burning (7.2%), construction (4.3%), industrial (3.3%), light-duty vehicles (5.4%), Pb (0.7%), Zn (0.7%), dust (22.1%), transported dust (9.5%), sulfates (15.4%), heavy-duty vehicles (17%), railway (6.6%) and fireworks (2.4%).

A study on oxidative potential apportionment of atmospheric PM_1 used a new approach combining high-sensitive online analysers (including the Xact) for chemical composition and offline PM oxidative potential (OP) measurement technique (Camman et al., 2024). Online measurements were conducted using the Xact, in parallel with a ToF-ACSM and an AE33, during summer (11 July – 1 September, 2018) in the urban background Marseille-Longchamp (MRS-LCP) supersite in the south of France. Six sources were identified from the Xact dataset: fireworks (2.3%), dust resuspension (53.7%), tire/brake wear (5.3%), regional background (23.4%), shipping (4.6%) and industrial emissions (10.7%). The factors of these elements were then used in a combined PMF with OA factors, non-refractory inorganics species and black carbon (1h resolution) to apportion the sources of the total PM_1 fraction. Finally, an inversion method was applied on factors issued from all PMFs to assess the contribution of the PM_1 sources to the OP measured from 4h filters.

Table 6. *Overview of published studies related to SA on Xact data in Europe. The PMF factors from the studies are categorized in main sources: Fireworks, Industrial, Salts, HFO (shipping), Dust, SIA, Traffic, Waste and Railway (contributions are provided in %). *: numbers non-provided in the publication.*

		Härkingen	**Veggiano**	**Pontardawe, Tawe Terrace**	**Zurich-Kaserne**	**Marseille-Longchamp**	**Prague**
Country		Switzerland	Italy	UK	Switzerland	France	Czech Republic
Reference		Rai et al. (2020)	Belis et al. (2019)	Font et al. (2022)	Manousakas et al. (2022)	Camman et al. (2024)	Windell et al. (2024)
PM inlet		PM10	PM2.5	PM10	PM10/PM2.5	PM1	PM2.5
Site typology		**Rural**	**SUB**	**Industrial**	**UB**	**UB**	**Traffic**
Period		Jul-Aug 2015	Jan-Feb 2015	Nov-Dec 2015	May 2019-May 2020	Jul-Aug 2018	Feb-Mar / Nov-Dec 2020
Fireworks		18.4			2.4	2.3	
Industrial		3	1.3	N* N N	0.7 0.7	10.7	
Salts	*Sea* *Road*	3.7		N	5.4		9
HFO (*shipping*)					3.3	4.6	
Dust	*Road* *Resuspension* *Transported*	16 18		N	26.4 9.5	53.7	21-31
SFC			36	N	7.2		20-39
SIA	*Sulfate* *Nitrate*	21	17 38	N	15.4	23.4	20-36
Traffic	*Non-exhaust* *Exhaust*	20	2	N	22.4	5.3	12-13
Waste treatment			3				
Railway					6.6		

Lastly, a study was conducted in a traffic site in Prague (Czech Republic) using the combination of online $PM_{2.5}$ metals from Xact and PM_1 elemental and organic carbon data with a 2h resolution. PMF was performed on this

combined dataset to resolve sources during spring (February–March) and winter (November–December) campaigns in 2020. The identified sources were mainly local, with local heating (39 and 20% for spring and winter, respectively), soil/road dust (21 and 31%) and traffic (12 and 13%). Besides these sources of local origin, a secondary inorganic aerosol factor was identified (20 and 36%) and a road salt factor (9%) only for spring.

In overall, these different SA studies could resolve similar sources of metals and elements but with elemental relative compositions varying depending on the size fraction of the measurements, the location of the sites and the list of elements used as inputs for the PMF analyses. An overview of these sources contributions is presented in Table 6 and Figure 10.

Sources such as traffic and SIA were found at all sites, accounting for non-exhaust and/or exhaust emissions, and ammonium sulfate and/or ammonium nitrate, respectively. Note that Camman et al. (2024) did not include sulphur to their PMF, but the so-called factor "Regional background" in Marseille was highly correlated with ammonium sulfate and included in this group in Table 6. Factors for industrial, salts, dust and SFC (Solid fuel combustion) were identified in every study, except for Prague; Veggiano and Marseille; Veggiano; and Härkingen and Marseille, respectively. Dust sources accounted for road dust, resuspended particles during the day (e.g., from construction) and transported dust (e.g., desert dust events), while salts include either marine sea salts or road salting. Fireworks from particular events (i.e., national celebrations) were quantified in the two Swiss sites in Zurich and Härkingen, and in Marseille in France. HFO (heavy fuel oil combustion) was only resolved at two sites: in Zurich, attributed to transported industrial emissions, and in Marseille, corresponding to the shipping emissions from the closed harbour. Finally, factors for waste thermal treatment and railway were resolved only in single studies, in Veggiano and Zurich, respectively.

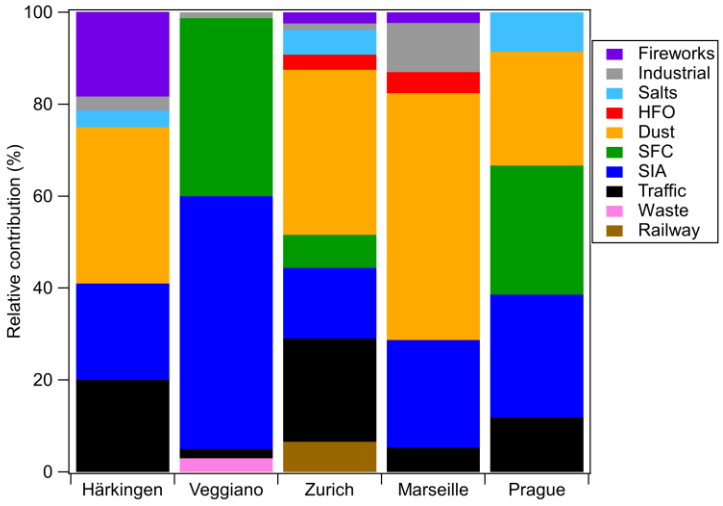

Figure 10. *Relative mean element composition of sites providing Xact source apportionment results.*

4.3 Recommendations for source apportionment based on high time resolution measurements of trace elements

Based on the previous results, some recommendations can be addressed for preparing input matrix and running PMF analyses for Xact datasets. Table 7 provides a full list of settings for data pre-treatment and PMF parameters.

- The mentioned studies performed PMF analyses on datasets including 12 to 25 elements. Some measured elements are usually excluded based on some criteria. Here, Font et al. (2022) and Windell et al. (2024) discarded the elements having bad signal-to-noise (S/N) ratio. Belis et al. (2019) removed elements showing bad correlations with offline analyses on filters. Rai et al. (2020), Manousakas et al. (2022) and Camman et al.

(2024) set thresholds for the amount of data below the detection limit (DL), with elements having >50% (and bad correlation with offline analyses), >70% and >90% of data below DL excluded from their analysis, respectively.

- It is of use to downweight (DW) observations (i.e. increase the uncertainty) which could badly affect the model. Belis et al. (2019), Font et al. (2022) and Windell et al. (2024) applied DW based on the averaged S/N of each variable, while Rai et al. (2020), Manousakas et al. (2022) and Camman et al. (2024) performed a DW cellwise as some variables which have low S/N on average can display high S/N during specific periods (Visser et al., 2015).
- In several studies, observations <DL are treated separately. Polissar et al. (1998) suggested to replace concentrations <DL with DL/2 and the associated uncertainties by 5/6 DL. This methodology was applied by all studies except the one of Font et al. (2022), where data inputs were reported without any modification, as recommended by (Brown et al., 2015). Manousakas et al. (2022) also applied this recommendation for data <DL (but not below or equal to 0), since replacing these values when the original measured values are available has no proven advantages when the elements with low S/N are downweighted in the modeling process.
- There are several methods for setting the matrix of uncertainties for Xact data. Belis et al. (2019), Font et al. (2022) and Windell et al. (2024) used directly the instrumental uncertainties provided by the Xact software, which account for uncertainties of the sampling volume and uncertainties of the mass spectra deconvolution. Rai et al. (2020) and Manousakas et al. (2022) used the methodology described by Reff et al. (2007) including the concentrations values, fixed analytical uncertainties of 10% and DL values. Camman et al. (2024) also applied this method but introduced the instrumental uncertainties as analytical uncertainties.
- In overall, all studies used a bootstrap resampling strategy to explore the rotational ambiguity and the stability of the PMF solutions.

Table 7. *Summary of PMF settings and data preparation from the six Xact SA studies in Europe.*

Location	*Reference*	*PM inlet*	*PMF inputs*	*Number of elements*	*Exclusion of elements*	*Downweigh t (DW)*	*Bootstraps*	*Uncertainty calculation*	*Datapoints <DL or <0*
Härkingen	Rai et al. (2020)	PM10	Only Xact	14	>50% below DL + bad correlation with offline	Y, cellwise S/N	Y	Reff et al. (2007)	Polissar et al. (1998)
Veggiano	Belis et al. (2019)	PM2.5	Combined with ACSM	12	Bad correlation with offline	Y, S/N of variables	Y	Instrument uncertainty	Polissar et al. (1998)
Pontardawe, Tawe Terrace	Font et al. (2022)	PM10	Only Xact	15	Bad S/N	Y, S/N of variables	Y	Instrument uncertainty	Unmodified
Zurich-Kaserne	Manousakas et al. (2022)	PM10/PM2.5	Only Xact with switching inlet	25	>70% below DL	Y, cellwise S/N	Y	Reff et al. (2007)	Polissar et al. (1998) only for 0/negative values
Marseille-Longchamp	Camman et al. (2024)	PM1	Combined with ACSM and AE33	19	>90% below DL	Y, cellwise S/N	Y	Reff et al. (2007) + Instrument uncertainty	Polissar et al. (1998)
Prague	Windell et al. (2024)	PM2.5	Combined with EC/OC	14	Bad S/N	Y, S/N of variables	Y	Instrument uncertainty	Polissar et al. (1998)

5. SOURCE APPORTIONMENT BASED ON DATASETS WITH DIFFERENT TIME-RESOLUTION

5.1 Methodology

Recently, there has been an increasing interest in comprehensive SA including aerosol species from different types of instruments. The combination of OA matrices and the rest of NR-PM_1 species was conducted and showed improved source identification with respect to the conventional OA SA (Zografou et al., 2022). Also, there are studies combining ACSM instrumentation with other instruments, e.g., aethalometer (Forello et al., 2019), X-ACT (Belis et al., 2019), offline filters (Srivastava et al., 2019), and VOCs (Kuo et al., 2014). The coupling of ACSM OA datasets with other instrumentation datasets was reported to be beneficial in terms of environmental feasibility of the sources studied.

It is important to highlight that a SA practice coupling instruments methodology has been expanded in the framework of RI-URBANS (Via et al., 2023). The multi-time resolution PMF was developed in Zhou et al. (2004) and was later embedded in the Source Finder software (SoFi Pro, Datalystica Ltd., Villigen, Switzerland; Canonaco et al., 2021). The highlight of this practice is the improvement of source description due to the more heuristic approach and their increased time resolution. However, in the case of some sources that are expected to be exclusive to certain instrument measurements, it would be advisable to perform PMF separately to avoid possible species' correlations within datasets mixing in the outcoming sources.

The coupling consists of an online plus offline dataset combination in a single PMF combining different time resolutions. As an example, in the Via et al. (2023) study they combined data of NR-PM_1 compounds from an ACSM and BC from an aethalometer of 30 min time resolution with 24 h resolution metals data from filters. These data were combined in a multi-time resolution (MTR) PMF analysis, preserving the highest time resolution (30 min) coherently with a sensitivity assessment previously conducted. That systematic evaluation showed the solution quality degradation when the higher time resolution datasets were averaged to meet the lower time resolution timestamps, both in terms of model residuals and environmental interpretability. For that reason, the recommendation for such cases is to avoid averaging datasets to match the several instrument timestamps and employ the multi-time resolution PMF instead, especially when the aforementioned sensitivity analysis is not conducted. This agrees with previous literature (Kuo et al., 2014; Belis et al., 2019). The MTR-PMF technique identified two more sources relative to the data coupling with the lowest time resolution (24 h) and four more with respect to the approach mimicking offline PMF, indicating that the combination of both high and low time data is significantly beneficial for SA.

This study also highlights the SA benefits of several instrumental measurements into a single PMF. For instance, the inclusion of industrial markers enabled the characterisation of the industry source, whose description with only NR-PM_1 compounds and BC species would have been less conclusive. This is also reported in Tong et al. (2022), which strongly recommend an uncertainty weighting assessment before coupling different instrumentations on a single PMF. This practice equates the weight of each dataset in PMF, avoiding the misrepresentation of a certain instrument species, and strongly influences the quality of source descriptions.

In conclusion, coupling different instrument data is generally a profitable practice for a more comprehensive SA. The multi-time resolution PMF is strongly advised for coupling instrumentation measurements of different time resolutions instead of averaging them to make the timestamps match, since it decreases the quality of the solution. It is also recommended to evaluate the uncertainty weightings of all the joined datasets to ensure equal representation on PMF.

5.2 Recommendations for source apportionment based on combined datasets

Based on the previous section, some recommendations can be addressed for preparing input matrix and running PMF analyses for multi-time resolution datasets.

- The use of multi-time resolution PMF is highly advised when the coupled instruments are expected to present comprehensive sources mixing all instrument species. If the outcoming sources are a priori expected to be non-coinciding, the recommendation is to perform PMF separately.
- Coupling of two or more instruments into a single dataset should be performed without altering the time resolution of these datasets, since it has been proven disadvantageous in terms of results quality and the multi-time resolution PMF equation ensures a proper entanglement of different timestamps.
- When coupling different instrumentations, a previous uncertainty weighting sensitivity study is advised, consisting of the evaluation of solution feasibility and model error as a function of the downweight of the uncertainties of the included instruments. This will provide a balanced representation of the species of each instrument in PMF running (Tong et al., 2022).

7. REFERENCES AND OTHER USEFUL LITERATURE

Albinet, A., Leoz-Garziandia, E., Budzinski, H., Villenave, E., 2006. Simultaneous analysis of oxygenated and nitrated polycyclic aromatic hydrocarbons on standard reference material 1649a (urban dust) and on natural ambient air samples by gas chromatography–mass spectrometry with negative ion chemical ionisation. J. Chromatogr., A 1121, 106–113, https://doi.org/10.1016/j.chroma.2006.04.043.

Albinet, A., Nalin, F., Tomaz, S., Beaumont, J., Lestremau, F., 2014. A simple QuEChERS-like extraction approach for molecular chemical characterization of organic aerosols: application to nitrated and oxygenated PAH derivatives (NPAH and OPAH) quantified by GC–NICIMS. Anal. Bioanal. Chem., 406, 3131–3148, https://doi.org/10.1007/s00216-014-7760-5.

Albinet, A., Tomaz, S., Lestremau, F., 2013. A really quick easy cheap effective rugged and safe (QuEChERS) extraction procedure for the analysis of particle-bound PAHs in ambient air and emission samples. Sci. Total Environ., 450-451, 31–38, https://doi.org/10.1016/j.scitotenv.2013.01.068.

Alier, M., Van Drooge, B.L., Dall'Osto, M., Querol, X., Grimalt, J.O., Tauler, R., 2013. Source apportionment of submicron organic aerosol at an urban background and a road site in Barcelona (Spain) during SAPUSS. Atmos. Chem. Phys., 13, 20, 10353-10371, https://doi.org/10.5194/acp-13-10353-2013.

Amato, F., Alastuey, A., Karanasiou, A., Lucarelli, F., Nava, S., Calzolai, G., Severi, M., Becagli, S., Gianelle, V.L., Colombi, C., Alves, C., Custódio, D., Nunes, T., Cerqueira, M., Pio, C., Eleftheriadis, K., Diapouli, E., Reche, C., Minguillón, M.C., Manousakas, M.-I., Maggos, T., Vratolis, S., Harrison, R.M., Querol, X., 2016. AIRUSE-LIFE+: A harmonized PM speciation and source apportionment in five southern European cities. Atmos. Chem. Phys., 16, 5, 3289-3309, https://doi.org/10.5194/acp-16-3289-2016.

Amato, F., Pandolfi, M., Escrig, A., Querol, X., Alastuey, A., Pey, J., Perez, N., Hopke, P.K., 2009. Quantifying road dust resuspension in urban environment by Multilinear Engine: A comparison with PMF2. Atmos. Environ., 43, 17, 2770-2780, https://doi.org/10.1016/j.atmosenv.2009.02.039.

Backman, J., Schmeisser, L., Virkkula, A., Ogren, J.A., Asmi, E., Starkweather, S., Sharma, S., Eleftheriadis, K., Uttal, T., Jefferson, A., Bergin, M., Makshtas, A., Tunved, P., Fiebig, M., 2017. On Aethalometer measurement uncertainties and an instrument correction factor for the Arctic. Atmos. Meas. Tech., 10, 5039–5062, https://doi.org/10.5194/amt-10-5039-2017.

Baduel, C., Voisin, D., Jaffrezo, J.L., 2010. Seasonal variations of concentrations and optical properties of water soluble HULIS collected in urban environments. Atmos. Chem. Phys., 10, 4085–4095, https://doi.org/10.5194/acp-10-4085-2010.

Baldasano, J.M., 2020. COVID-19 lockdown effects on air quality by NO2 in the cities of Barcelona and Madrid (Spain). Sci. Total Environ., 741, https://doi.org/10.1016/j.scitotenv.2020.140353.

Becerril-Valle, M., Coz, E., Prévôt, A.S.H., Močnik, G., Pandis, S.N., Sánchez de la Campa, A.M., Alastuey, A., Díaz, E., Pérez, R.M., Artíñano, B., 2017. Characterization of atmospheric black carbon and co-pollutants in urban and rural areas of Spain. Atmos. Environ., 169, 36–53, https://doi.org/10.1016/j.atmosenv.2017.09.014.

Belis, C. A., M. Pikridas, F. Lucarelli, E. Petralia, F. Cavalli, G. Calzolai, M. Berico, and J. Sciare. 2019. Source Apportionment of Fine PM by Combining High Time Resolution Organic and Inorganic Chemical Composition Datasets. Atmos. Environ.: X 3, 100046, https://doi.org/10.1016/j.aeaoa.2019.100046.

Belis, C., Favez, O., Mircea, M., Diapouli, E., Manousakas, M., Vratolis, S., Gilardoni, S., Paglione, M., Decesari, S., Mocnik, G., Mooibroek, D., Salvador, P., Takahama, S., Vecchi, R. and Paatero, P., 2019. European guide on air pollution source apportionment with receptor models, EUR 29816 EN, Publications Office of the European Union, Luxembourg, 2019, ISBN 978-92-76-09001-4, https://doi:10.2760/439106, JRC117306.

Belis, C.A., Karagulian, F., Larsen, B.R., Hopke, P.K., 2013. Critical review and meta-analysis of ambient particulate matter source apportionment using receptor models in Europe. Atmos. Environ. 69, 94–108, https://doi.org/10.1016/j.atmosenv.2012.11.009.

Bibi, Z., Coe, H., Brooks, J., Williams, P.I., Reyes-Villegas, E., Priestley, M., Percival, C.J., Allan, J.D., 2021. Technical note: A new approach to discriminate different black carbon sources by utilising fullerene and metals in positive matrix factorisation analysis of high-resolution soot particle aerosol mass spectrometer data. Atmos. Chem. Phys., 21, 10763–10777, https://doi.org/10.5194/acp-21-10763-2021.

Blanco-Donado, E.P., Schneider, I.L., Artaxo, P., Lozano-Osorio, J., Portz, L., Oliveira, M.L.S., 2022. Source identification and global implications of black carbon. Geosci. Front. 13, 101149, https://doi.org/10.1016/j.gsf.2021.101149.

Bressi, M., Cavalli, F., Putaud, J. P., Fröhlich, R., Petit, J. E., Aas, W., Äijälä, M., Alastuey, A., …, Prevot, A. S. H., 2001. A European aerosol phenomenology - 7: High-time resolution chemical characteristics of submicron particulate matter across Europe, Atmos. Environ., X 10, https://doi:10.1016/j.aeaoa.2021.100108.

Briggs, N.L., Long, C.M., 2016. Critical review of black carbon and elemental carbon source apportionment in Europe and the United States. Atmos. Environ., 144, 409–427, https://doi.org/10.1016/j.atmosenv.2016.09.002.

Brown, S.G., Eberly, S., Paatero, P., Norris, G.A., 2015. Methods for estimating uncertainty in PMF solutions: Examples with ambient air and water quality data and guidance on reporting PMF results. Sci. Total Environ., 518-519, 626-635, https://doi.org/10.1016/j.scitotenv.2015.01.022.

Camman, J., Chazeau, B., Marchand, N., Durand, A., Gille, G., Lanzi, L., Jaffrezo, J.-L., Wortham, H., and Uzu, G., 2024. Oxidative potential apportionment of atmospheric PM1: A new approach combining high-sensitive online analysers for chemical composition and offline OP measurement technique, Atmos. Chem. Phys., 24, 3257–3278, https://doi.org/10.5194/acp-24-3257-2024.

Canonaco, F., Slowik, J. G., Baltensperger, U. and Prévôt, A. S. H.: Seasonal differences in oxygenated organic aerosol composition, 2015. Implications for emissions sources and factor analysis, Atmos. Chem. Phys., 15, 12, 6993–7002, https://doi:10.5194/acp-15-6993-2015.

Canonaco, F., Tobler, A., Chen, G., Sosedova, Y., Slowik, J. G., Bozzetti, C., ... & Prévôt, A. S. H., 2021. A new method for long-term source apportionment with time-dependent factor profiles and uncertainty assessment using SoFi Pro: application to 1 year of organic aerosol data. Atmos. Meas. Techn., 14, 2, 923-943, https://doi.org/10.5194/amt-14-923-2021.

Cavalli, F., Viana, M., Yttri, K., Genberg, J., Putaud, J.-P., 2010. Toward a standardised thermal-optical protocol for measuring atmospheric organic and elemental carbon: the EUSAAR protocol. Atmos. Meas. Tech. 3, 79–89, https://doi.org/10.5194/amt-3-79-2010.

Cesari, D., Amato, F., Pandolfi, M., Alastuey, A., Querol, X., Contini, D., 2016. An inter-comparison of PM10 source apportionment using PCA and PMF receptor models in three European sites. Environ. Sci. Poll. Res., 23, 15, 15133-15148, https://doi.org/10.1007/s11356-016-6599-z.

Chazeau, B., El Haddad, I., Canonaco, F., Temime-Roussel, B., D'Anna, B., Gille, G., Mesbah, B., Prévôt, A.S.H., Wortham, H., Marchand, N., 2022. Organic aerosol source apportionment by using rolling positive matrix factorization: Application to a Mediterranean coastal city. Atmos. Environ. X 14, https://doi.org/10.1016/j.aeaoa.2022.100176.

Chebaicheb, H., Brito, J.F. De, Chen, G., Tison, E., Favez, O., Marchand, C., Pr, S.H., 2023. Investigation of four-year chemical composition and organic aerosol sources of submicron particles at the ATOLL site in northern France. Environ. Poll., 330, 121805, https://doi.org/10.1016/j.envpol.2023.121805.

Chen, G., Canonaco, F., Tobler, A., Aas, W., Alastuey, A., Allan, J., Atabakhsh, S., ..., Prévôt, A. S. H., 2022a. European aerosol phenomenology − 8: Harmonised source apportionment of organic aerosol using 22 Year-long ACSM/AMS datasets, Environ. Int., 166, 107325, https://doi.org/10.1016/j.envint.2022.107325.

Chen, G., Canonaco, F., Slowik, J. G., Daellenbach, K. R., Tobler, A., Petit, J. E., Favez, O., Stavroulas, I., Mihalopoulos, N., Gerasopoulos, E., El Haddad, I., Baltensperger, U., Prévôt, A. S., 2022b. Real-time source apportionment of organic aerosols in three european cities. Environ. Sci. Tech., 56, 22, 15290-15297, https://doi.org/10.1021/acs.est.2c02509.

Christodoulou, A., Stavroulas, I., Vrekoussis, M., Desservettaz, M., Pikridas, M., Bimenyimana, E., Kushta, J., Ivančič, M., Rigler, M., Goloub, P., Oikonomou, K., Sarda-Estève, R., Savvides, C., Afif, C., Mihalopoulos, N., Sauvage, S., & Sciare, J., 2023. Ambient carbonaceous aerosol levels in Cyprus and the role of pollution transport from the Middle East. Atmos. Chem. Phys., *23*, 11, 6431-6456, https://doi.org/10.5194/acp-23-6431-2023.

Cordell, R.L., Mazet, M., Dechoux, C., Hama, S.M.L., Staelens, J., Hofman, J., Stroobants, C., Roekens, E., Kos, G.P.A., Weijers, E.P., Frumau, K.F.A., Panteliadis, P., Delaunay, T., Wyche, K.P., Monks, P.S., 2016. Evaluation of biomass burning across North West Europe and its impact on air quality. Atmos. Environ., 141, 276–286, https://doi.org/10.1016/j.atmosenv.2016.06.065.

Crespi, A., Bernardoni, V., Calzolai, G., Lucarelli, F., Nava, S., Valli, G. and Vecchi, R., 2016. Implementing constrained multi-time approach with bootstrap analysis in ME-2: An application to PM2.5 data from Florence (Italy), Sci. Total Environ., 541, 502–511, https://doi:10.1016/j.scitotenv.2015.08.159.

Crilley, L.R., Bloss, W.J., Yin, J., Beddows, D.C.S., Harrison, R.M., Allan, J.D., Young, D.E., Flynn, M., Williams, P., Zotter, P., Prevot, A.S.H., Heal, M.R., Barlow, J.F., Halios, C.H., Lee, J.D., Szidat, S., Mohr, C., 2015. Sources and contributions of wood smoke during winter in London: Assessing local and regional influences. Atmos. Chem. Phys. 15, 3149–3171, https://doi.org/10.5194/acp-15-3149-2015.

Crippa, M., Canonaco, F., Lanz, V. A., Äijälä, M., Allan, J. D., Carbone, S., Capes, G., Ceburnis, …, Prévôt, A. S. H., 2014. Organic aerosol components derived from 25 AMS data sets across Europe using a consistent ME-2 based source apportionment approach, Atmos. Chem. Phys., 14, 12, 6159–6176, https://doi:10.5194/acp-14-6159-2014.

Duan, J., Huang, R. J., Li, Y., Chen, Q., Zheng, Y., Chen, Y., ... & Cao, J. (2020). Summertime and wintertime atmospheric processes of secondary aerosol in Beijing. Atmospheric Chemistry and Physics, 20(6), 3793-3807.

El Haddad, I., D'Anna, B., Temime-Roussel, B., Nicolas, M., Boreave, A., Favez, O., Voisin, D., Sciare, J., George, C., Jaffrezo, J.L., Wortham, H., Marchand, N., 2013. Towards a better understanding of the origins, chemical composition and aging of oxygenated organic aerosols: Case study of a Mediterranean industrialized environment, Marseille. Atmos. Chem. Phys., 13, 7875–7894. https://doi.org/10.5194/acp-13-7875-2013.

Favez, O., Cachier, H., Sciare, J., Sarda-Estève, R., Martinon, L., 2009. Evidence for a significant contribution of wood burning aerosols to PM2.5 during the winter season in Paris, France. Atmos. Environ. 43, 3640–3644, https://doi.org/10.1016/j.atmosenv.2009.04.035.

Favez, O., El Haddad, I., Piot, C., Boréave, A., Abidi, E., Marchand, N., Jaffrezo, J.L., Besombes, J.L., Personnaz, M.B., Sciare, J., Wortham, H., George, C., D'Anna, B., 2010. Inter-comparison of source apportionment models for the estimation of wood burning aerosols during wintertime in an Alpine city (Grenoble, France). Atmos. Chem. Phys., 10, 5295–5314, https://doi.org/10.5194/acp-10-5295-2010.

Favez, O., El Haddad, I., Piot, C., Boréave, A., Abidi, E., Marchand, N., Jaffrezo, J.L., Besombes, J.L., Personnaz, M.B., Sciare, J., Wortham, H., George, C., D'Anna, B., 2010. Inter-comparison of source apportionment models for the estimation of wood burning aerosols during wintertime in an alpine city (Grenoble, France). Atmos. Chem. Phys. 10, 5295–5314, https://doi.org/10.5194/acp-10-5295-2010.

Ferrero, L., Bernardoni, V., Santagostini, L., Cogliati, S., Soldan, F., Valentini, S., Massabò, D., Močnik, G., Gregorič, A., Rigler, M., Prati, P., Bigogno, A., Losi, N., Valli, G., Vecchi, R., Bolzacchini, E., 2021. Consistent determination

of the heating rate of light-absorbing aerosol using wavelength- and time-dependent Aethalometer multiple-scattering correction. Sci. Total Environ., 791, https://doi.org/10.1016/j.scitotenv.2021.148277.

Font, Anna, Anja H. Tremper, Max Priestman, Frank J. Kelly, Francesco Canonaco, André S.H. Prévôt, and David C. Green. 2022. Source Attribution and Quantification of Atmospheric Nickel Concentrations in an Industrial Area in the United Kingdom (UK). Environ. Poll., 293, https://doi.org/10.1016/j.envpol.2021.118432.

Fontal, M., van Drooge, B.L., López, J.F., Fernández, P., Grimalt, J.O., 2015. Broad spectrum analysis of polar and apolar organic compounds in submicron atmospheric particles. J. Chromatogr. A, 1404, 28-38, https://doi.org/10.1016/j.chroma.2015.05.042.

Forello, A. C., Bernardoni, V., Calzolai, G., Lucarelli, F., Massabò, D., Nava, S., Pileci, R. E., Prati, P., Valentini, S., Valli, G. and Vecchi, R., 2019. Exploiting multi-wavelength aerosol absorption coefficients in a multi-time source apportionment study to retrieve source-dependent absorption parameters, Atmos. Chem. Phys., 19, 17, 11235-11252, https://doi.org/10.5194/acp-19-11235-2019.

Fourtziou, L., Liakakou, E., Stavroulas, I., Theodosi, C., Zarmpas, P., Psiloglou, B., Sciare, J., Maggos, T., Bairachtari, K., Bougiatioti, A., Gerasopoulos, E., Sarda-Estève, R., Bonnaire, N., Mihalopoulos, N., 2017. Multi-tracer approach to characterize domestic wood burning in Athens (Greece) during wintertime. Atmos. Environ., 148, 89–101, https://doi.org/10.1016/j.atmosenv.2016.10.011.

Fung, P.L., Sillanpää, S., Niemi, J. V., Kousa, A., Timonen, H., Zaidan, M.A., Saukko, E., Kulmala, M., Petäjä, T., Hussein, T., 2022. Improving the current air quality index with new particulate indicators using a robust statistical approach. Sci. Total Environ., 844, https://doi.org/10.1016/j.scitotenv.2022.157099.

Furger, Markus, María Cruz Minguillón, Varun Yadav, Jay G. Slowik, Christoph Hüglin, Roman Fröhlich, Krag Petterson, Urs Baltensperger, and André S.H. Prévôt. 2017. Elemental Composition of Ambient Aerosols Measured with High Temporal Resolution Using an Online XRF Spectrometer. Atmos. Meas. Tech., 10, 6, 2061–76, https://doi.org/10.5194/amt-10-2061-2017.

Furger, Markus, Pragati Rai, Jay G. Slowik, Junji Cao, Suzanne Visser, Urs Baltensperger, and André S.H. Prévôt. 2020. Automated Alternating Sampling of PM10 and PM2.5 with an Online XRF Spectrometer. Atmos. Environ. X 5, https://doi.org/10.1016/j.aeaoa.2020.100065.

Garg, S., Chandra, B.P., Sinha, V., Sarda-Esteve, R., Gros, V., Sinha, B., 2016. Limitation of the Use of the Absorption Angstrom Exponent for Source Apportionment of Equivalent Black Carbon: A Case Study from the North West Indo-Gangetic Plain. Environ. Sci. Technol., 50, 814–824, https://doi.org/10.1021/acs.est.5b03868.

Grange, S., Lötscher, H., Fischer, A., Emmenegger, L., Hueglin, C., 2020. Evaluation of equivalent black carbon source apportionment using observations from Switzerland between 2008 and 2018. Atmos. Meas. Tech., 13, 1867–1885. https://doi.org/10.5194/amt-13-1867-2020.

Gregorič, A., Drinovec, L., JeÅ3/4ek, I., Vaupotič, J., Grauf, D., Wang, L., Stanič, S., 2020. The determination of highly time-resolved and source-separated black carbon emission rates using radon as a tracer of atmospheric dynamics. Atmos. Chem. Phys., 20, 14139–14162, https://doi.org/10.5194/acp-20-14139-2020.

Hamilton, S.D., Harley, R.A., 2021. High-Resolution Modeling and Apportionment of Diesel-Related Contributions to Black Carbon Concentrations. Environ. Sci. Technol. 55, 12250–12260, https://doi.org/10.1021/acs.est.1c03913.

Harrison, R.M., Beddows, D.C.S., Jones, A.M., Calvo, A., Alves, C., Pio, C., 2013. An evaluation of some issues regarding the use of aethalometers to measure woodsmoke concentrations. Atmos. Environ., 80, 540–548, https://doi.org/10.1016/j.atmosenv.2013.08.026.

Hasheminassab, Sina, Mohammad H. Sowlat, Payam Pakbin, Aaron Katzenstein, Jason Low, and Andrea Polidori. 2020. High Time-Resolution and Time-Integrated Measurements of Particulate Metals and Elements in an Environmental Justice Community within the Los Angeles Basin: Spatio-Temporal Trends and Source Apportionment. Atmos. Environ. X 7, 100089, https://doi.org/10.1016/j.aeaoa.2020.100089.

Helin, A., Niemi, J. V., Virkkula, A., Pirjola, L., Teinilä, K., Backman, J., Aurela, M., Saarikoski, S., Rönkkö, T., Asmi, E., Timonen, H., 2018. Characteristics and source apportionment of black carbon in the Helsinki metropolitan area, Finland. Atmos. Environ. 190, 87–98, https://doi.org/10.1016/j.atmosenv.2018.07.022.

Helin, A., Virkkula, A., Backman, J., Pirjola, L., Sippula, O., Aakko-Saksa, P., Väätäinen, S., Mylläri, F., Järvinen, A., Bloss, M., Aurela, M., Jakobi, G., Karjalainen, P., Zimmermann, R., Jokiniemi, J., Saarikoski, S., Tissari, J., Rönkkö, T., Niemi, J. V., Timonen, H., 2021. Variation of Absorption Ångström Exponent in Aerosols from Different Emission Sources. J. Geophys. Res. Atmos., 126, 1–21, https://doi.org/10.1029/2020JD034094.

Herich, H., Hueglin, C., Buchmann, B., 2011. A 2.5 year's source apportionment study of black carbon from wood burning and fossil fuel combustion at urban and rural sites in Switzerland. Atmos. Meas. Tech., 4, 1409–1420,https://doi.org/10.5194/amt-4-1409-2011.

Hopke, P. K., 2020. A guide to positive matrix factorization, US-EPA, 16p, https://www3.epa.gov/ttnamti1/files/ambient/pm25/workshop/laymen.pdf.

Hopke, P.K., 2016. Review of receptor modeling methods for source apportionment. J. Air Waste Manag. Assoc., 66, 237–259, https://doi.org/10.1080/10962247.2016.1140693.

Hopke, P.K., Chen, Y., Rich, D.Q., Mooibroek, D., Sofowote, U.M., 2023. Chemometrics and Intelligent Laboratory Systems The application of positive matrix factorization with diagnostics to BIG DATA. Chemom. Intell. Lab. Syst. 240, 104885, https://doi.org/10.1016/j.chemolab.2023.104885.

Hu, Q. H., Xie, Z. Q., Wang, X. M., Kang, H. and Zhang, P.: Levoglucosan indicates high levels of biomass burning aerosols over oceans from the Arctic to Antarctic, Sci. Rep., 3, 1–7, https://doi:10.1038/srep03119, 2013.

Hyvärinen, A.P., Kolmonen, P., Kerminen, V.M., Virkkula, A., Leskinen, A., Komppula, M., Hatakka, J., Burkhart, J., Stohl, A., Aalto, P., Kulmala, M., Lehtinen, K.E.J., Viisanen, Y., Lihavainen, H., 2011. Aerosol black carbon at five background measurement sites over Finland, a gateway to the Arctic. Atmos. Environ., 45, 4042–4050, https://doi.org/10.1016/j.atmosenv.2011.04.026.

Jafar, H.A., Harrison, R.M., 2021. Spatial and temporal trends in carbonaceous aerosols in the United Kingdom. Atmos. Pollut. Res., 12, 295–305, https://doi.org/10.1016/j.apr.2020.09.009.

Jaffrezo, J.L., Aymoz, G., Delaval, C., Cozic, J., 2005. Seasonal variations of the water-soluble organic carbon mass fraction of aerosol in two valleys of the French Alps. Atmos. Chem. Phys., 5, 2809–2821. https://doi.org/10.5194/acp-5-2809-2005.

Kaskaoutis, D.G., Grivas, G., Stavroulas, I., Bougiatioti, A., Liakakou, E., Dumka, U.C., Gerasopoulos, E., Mihalopoulos, N., 2021. Apportionment of black and brown carbon spectral absorption sources in the urban environment of Athens, Greece, during winter. Sci. Total Environ., 801, 149739, https://doi.org/10.1016/j.scitotenv.2021.149739.

Krecl, P., Johansson, C., Targino, A.C., Ström, J., Burman, L., 2017. Trends in black carbon and size-resolved particle number concentrations and vehicle emission factors under real-world conditions. Atmos. Environ., 165, 155–168, https://doi.org/10.1016/j.atmosenv.2017.06.036.

Krecl, P., Targino, A.C., Johansson, C., 2011. Spatiotemporal distribution of light-absorbing carbon and its relationship to other atmospheric pollutants in Stockholm. Atmos. Chem. Phys. 11, 11553–11567, https://doi.org/10.5194/acp-11-11553-2011.

Kumar, S., Wang, S., Lin, N., Chantara, S., Lee, C., Thepnuan, D., 2020. Black carbon over an urban atmosphere in northern peninsular Southeast Asia: Characteristics, source apportionment, and associated health risks. Environ. Pollut., 259, 113871. https://doi.org/10.1016/j.envpol.2019.113871.

Kuo, C.-P., Liao, H.-T., Chou, C.C.-K., Wu, C.-F., 2014. Source apportionment of particulate matter and selected volatile organic compounds with multiple time resolution data. Sci. Total Environ., 472, 880-887., https://doi.org/10.1016/j.scitotenv.2013.11.114.

Kutzner, R.D., von Schneidemesser, E., Kuik, F., Quedenau, J., Weatherhead, E.C., Schmale, J., 2018. Long-term monitoring of black carbon across Germany. Atmos. Environ., 185, 41–52, https://doi.org/10.1016/j.atmosenv.2018.04.039.

Laborde, M., Crippa, M., Tritscher, T., Jurányi, Z., Decarlo, P.F., Temime-Roussel, B., Marchand, N., Eckhardt, S., Stohl, A., Baltensperger, U., Prévôt, A.S.H., Weingartner, E., Gysel, M., 2013. Black carbon physical properties and mixing state in the European megacity Paris. Atmos. Chem. Phys., 13, 5831–5856, https://doi.org/10.5194/acp-13-5831-2013.

Lee, E., Chan, C. K., and Paatero, P., 1999 Application of positive matrix factorization in source apportionment of particulate pollutants in Hong Kong, Atmos. Environ., 33, 3201–3212, https://doi.org/10.1016/S1352-2310(99)00113-2.

Li, J., Liu, C., Yin, Y., Kumar, K.R., 2016. Numerical investigation on the Ångström exponent of black carbon aerosol. J. Geophys. Res. Atmos. 121, 3506–3518. https://doi.org/10.1002/2015jd024718.

Lin, C., Ceburnis, D., Trubetskaya, A., Xu, W., Smith, W., Hellebust, S., ... & Ovadnevaite, J., 2021. On the use of reference mass spectra for reducing uncertainty in source apportionment of solid-fuel burning in ambient organic aerosol. Atmos. Meas. Tech., 14, 10, 6905-6916, https://doi.org/10.5194/amt-14-6905-2021.

Liakakou, E., Stavroulas, I., Kaskaoutis, D.G., Grivas, G., Paraskevopoulou, D., Dumka, U.C., Tsagkaraki, M., Bougiatioti, A., Oikonomou, K., Sciare, J., Gerasopoulos, E., Mihalopoulos, N., 2020. Long-term variability, source apportionment and spectral properties of black carbon at an urban background site in Athens, Greece. Atmos. Environ., 222, 117137, https://doi.org/10.1016/j.atmosenv.2019.117137.

Liu, C., Chung, C.E., Yin, Y., Schnaiter, M., 2018. The absorption Ångström exponent of black carbon: From numerical aspects. Atmos. Chem. Phys., 18, 6259–6273, https://doi.org/10.5194/acp-18-6259-2018.

Liu, X., Zheng, M., Liu, Y., Jin, Y., Liu, J., Zhang, B., Yang, X., Wu, Y., Zhang, T., Xiang, Y., Liu, B., Yan, C., 2022. Intercomparison of equivalent black carbon (eBC) and elemental carbon (EC) concentrations with three-year continuous measurement in Beijing, China. Environ. Res., 209, 112791, https://doi.org/10.1016/j.envres.2022.112791.

Liu, Yue, Mei Zheng, Mingyuan Yu, Xuhui Cai, Huiyun Du, Jie Li, Tian Zhou, et al. 2019. High-Time-Resolution Source Apportionment of PM2.5 in Beijing with Multiple Models. Atmos. Phys. Chem., 19, 9, 6595–6609, https://doi.org/10.5194/acp-19-6595-2019.

Luo, J., Li, Z., Qiu, J., Zhang, Y., Fan, C., Li, L., Wu, H., Zhou, P., Li, K., Zhang, Q., 2023. The Simulated Source Apportionment of Light Absorbing Aerosols: Effects of Microphysical Properties of Partially-Coated Black Carbon. J. Geophys. Res. Atmos, 128, https://doi.org/10.1029/2022JD037291.

Luoma, K., Niemi, J. V., Aurela, M., Lun Fung, P., Helin, A., Hussein, T., Kangas, L., Kousa, A., Rönkkö, T., Timonen, H., Virkkula, A., Petäjä, T., 2021. Spatiotemporal variation and trends in equivalent black carbon in the Helsinki metropolitan area in Finland. Atmos. Chem. Phys., 21, 1173–1189, https://doi.org/10.5194/acp-21-1173-2021.

Lyamani, H., Olmo, F.J., Foyo, I., Alados-Arboledas, L., 2011. Black carbon aerosols over an urban area in south-eastern Spain: Changes detected after the 2008 economic crisis. Atmos. Environ., 45, 6423–6432, https://doi.org/10.1016/j.atmosenv.2011.07.063.

Manousakas, M, E Diapouli, C A Belis, V Vasilatou, M Gini, F Lucarelli, X Querol, and K Eleftheriadis. 2021. Quantitative Assessment of the Variability in Chemical Profiles from Source Apportionment Analysis of PM10 and PM2.5 at Different Sites within a Large Metropolitan Area. Environ. Res., 192, 110257, https://doi.org/10.1016/j.envres.2020.110257.

Manousakas, M, M Furger, K R Daellenbach, F Canonaco, G Chen, A Tobler, P Rai, et al. 2022. Source Identification of the Elemental Fraction of Particulate Matter Using Size Segregated, Highly Time-Resolved Data and an Optimized Source Apportionment Approach. Atmos. Environ X 14, 100165, https://doi.org/10.1016/j.aeaoa.2022.100165.

Mărmureanu, L., Vasilescu, J., Slowik, J., Prévôt, A.S.H., Marin, C.A., Antonescu, B., Vlachou, A., Nemuc, A., Dandocsi, A., Szidat, S., 2020. Online Chemical Characterization and Source Identification of Summer and Winter Aerosols in Măgurele, Romania. Atmosphere, 11, *385, https*://doi.org/10.3390/atmos11040385.

Masiol, M., Squizzato, S., Rich, D.Q., Hopke, P.K., 2019. Long-term trends (2005–2016) of source apportioned PM2.5 across New York State. Atmos. Environ., 201, 110–120, https://doi.org/10.1016/j.atmosenv.2018.12.038.

Massabò, D., Prati, P., 2021. An overview of optical and thermal methods for the characterization of carbonaceous aerosol, Rivista del Nuovo Cimento. Springer Berlin Heidelberg, https://doi.org/10.1007/s40766-021-00017-8.

Mbengue, S., Serfozo, N., Schwarz, J., Holoubek, I., Ziková, N., Šmejkalová, A.H., Holoubek, I., 2020. Characterization of Equivalent Black Carbon at a regional background site in Central Europe: Variability and source apportionment☆. Environ. Pollut., 260, https://doi.org/10.1016/j.envpol.2019.113771.

Merabet, H., Kerbachi, R., Mihalopoulos, N., Stavroulas, I., Kanakidou, M., Yassaa, N., 2019. Measurement of atmospheric black carbon in some south mediterranean cities: Seasonal variations and source apportionment. Clean Air J., 29, 1–19, https://doi.org/10.17159/caj/2019/29/2.7500.

Milinković, A., Gregorič, A., Grgičin, V.D., Vidič, S., Penezić, A., Kušan, A.C., Alempijević, S.B., Kasper-Giebl, A., Frka, S., 2021. Variability of black carbon aerosol concentrations and sources at a Mediterranean coastal region. Atmos. Pollut. Res., 12, https://doi.org/10.1016/j.apr.2021.101221.

Minderytė, A., Pauraite, J., Dudoitis, V., Plauškaitė, K., Kilikevičius, A., Matijošius, J., Rimkus, A., Kilikevičienė, K., Vainorius, D., Byčenkienė, S., 2022. Carbonaceous aerosol source apportionment and assessment of transport-related pollution. Atmos. Environ., 279, https://doi.org/10.1016/j.atmosenv.2022.119043.

Mousavi, A., Sowlat, M.H., Hasheminassab, S., Polidori, A., Sioutas, C., 2018. Spatio-temporal trends and source apportionment of fossil fuel and biomass burning black carbon (BC) in the Los Angeles Basin. Sci. Total Environ., 640–641, 1231–1240, https://doi.org/10.1016/j.scitotenv.2018.06.022.

Mousavi, A., Sowlat, M.H., Lovett, C., Rauber, M., Szidat, S., Bo, R., Borgini, A., Marco, C. De, Ruprecht, A.A., Sioutas, C., Boffi, R., Borgini, A., De Marco, C., Ruprecht, A.A., Sioutas, C., Bo, R., Borgini, A., Marco, C. De, Ruprecht, A.A., Sioutas, C., 2019. Source apportionment of black carbon (BC) from fossil fuel and biomass burning in metropolitan Milan, Italy. Atmos. Environ., 203, 252–261, https://doi.org/10.1016/j.atmosenv.2019.02.009.

Ng, N.L., Canagaratna, M.R., Jimenez, J.L., Zhang, Q., , Ulbrich, I.M., Worsnop, D.R., 2011. Real-Time Methods for Estimating Organic Component Mass Concentrations from Aerosol Mass Spectrometer Data. Environ. Sci. Technol., 45, 3, 910–916, https://doi.org/10.1021/es102951k.

Nozière, B., Kalberer, M., Claeys, M., Allan, J., D'Anna, B., Decesari, S., Finessi, E., Glasius, M., …., Wisthaler, A., 2015. The molecular identification of organic compounds in the atmosphere: state of the art and challenges. Chem. Rev., 115, 3919–3983, https://doi.org/10.1021/cr5003485.

Paatero, P., Hopke, P.K., 2003. Discarding or downweighting high-noise variables in factor analytic models. Anal. Chim. Acta, 490, 277–289, https://doi.org/10.1016/S0003-2670(02)01643-4.

Paatero, P., & Hopke, P. K., 2009. Rotational tools for factor analytic models. J. Chemometrics, 23, 2, 91-100. https://doi.org/10.1002/cem.1197.

Paglione, M., Gilardoni, S., Rinaldi, M., Decesari, S., Zanca, N., Sandrini, S., ... & Fuzzi, S. (2020). The impact of biomass burning and aqueous-phase processing on air quality: a multi-year source apportionment study in the Po Valley, Italy. Atmos. Chem. Phys., 20, 3, 1233-1254, https://doi.org/10.5194/acp-20-1233-2020.

Pandolfi, M., Ripoll, A., Querol, X., Alastuey, A., 2014. Climatology of aerosol optical properties and black carbon mass absorption cross section at a remote high-altitude site in the western Mediterranean Basin. Atmos. Chem. Phys., 14, 6443–6460, https://doi.org/10.5194/acp-14-6443-2014.

Pauraitė, J., Mordas, G., Byčenkienė, S., & Ulevicius, V., 2015. Spatial and temporal analysis of organic and black carbon mass concentrations in Lithuania. Atmosphere, 6, 8, 1229-1242, https://doi.org/10.3390/atmos6081229

Petit, J. E., Favez, O., Sciare, J., Canonaco, F., Croteau, P., Močnik, G., Jayne, J., Worsnop, D. and Leoz-Garziandia, E., 2014. Submicron aerosol source apportionment of wintertime pollution in Paris, France by double positive matrix factorization (PMF2) using an aerosol chemical speciation monitor (ACSM) and a multi-wavelength Aethalometer, Atmos. Chem. Phys., 14, 24, 13773–13787, https://doi:10.5194/acp-14-13773-2014.

Querol X., Alastuey A., Rodriguez S., Plana F., Mantilla E., Ruiz C.R., 2001. Monitoring of PM10 and PM2.5 around primary particulate anthropogenic emission sources. Atmos. Environ., 35, 5, 845-858, https://doi.org/10.1016/S1352-2310(00)00387-3.

Rai, Pragati, Jay G Slowik, Markus Furger, Imad El Haddad, Suzanne Visser, Yandong Tong, Atinderpal Singh, et al. 2021. Highly Time-Resolved Measurements of Element Concentrations in PM10 and PM 2.5: Comparison of Delhi, Beijing, London, and Krakow. Atmos. Chem. Phys., 21, 717–30, https://doi.org/10.5194/acp-21-717-2021.

Rai, Pragati, Markus Furger, Imad El Haddad, Varun Kumar, Liwei Wang, Atinderpal Singh, Kuldeep Dixit, et al. 2020. Real-Time Measurement and Source Apportionment of Elements in Delhi's Atmosphere. Sci. Total Environ., 742, 140332, https://doi.org/10.1016/j.scitotenv.2020.140332.

Rai, Pragati, Markus Furger, Jay Slowik, Francesco Canonaco, Roman Fröhlich, Christoph Hüglin, María Cruz Minguillón, Krag Petterson, Urs Baltensperger, and André S. H. Prévôt. 2019. Source Apportionment of Highly Time Resolved Trace Elements during a Firework Episode from a Rural Freeway Site in Switzerland. Atmos. Chem. Phys., 19, 1–25, https://doi.org/10.5194/acp-2018-1229.

Reimann, S., Wegener, R., Claude, A., and Sauvage, S., 2020. ACTRIS' Milestone 3.10. Released Measurement Guideline for VOCs and NOx, 2p, www.actris.eu/sites/default/files/Documents/ACTRIS-2/Milestones/WP3_MS3.10.pdf.

Rivas, I., Beddows, D.C.S., Amato, F., Green, D.C., Järvi, L., Hueglin, C., Reche, C., Timonen, H., Fuller, G.W., Niemi, J. V., Pérez, N., Aurela, M., Hopke, P.K., Alastuey, A., Kulmala, M., Harrison, R.M., Querol, X., Kelly, F.J., 2020. Source apportionment of particle number size distribution in urban background and traffic stations in four European cities. Environ. Int., 135, 105345, https://doi.org/10.1016/j.envint.2019.105345.

Rusanen, A., Björklund, A., Manousakas, M.I., Jiang, J., Kulmala, M.T., Puolamäki, K., & Daellenbach, K.R., 2024. A novel probabilistic source apportionment approach: Bayesian auto-correlated matrix factorization. Atmos. Meas. Texch., *17*, 4, 1251-1277, https://doi.org/10.5194/amt-17-1251-2024.

Salameh, D., Pey, J., Bozzetti, C., El Haddad, I., Detournay, A., Sylvestre, A., Canonaco, F., Armengaud, A., Piga, D., Robin, D., Prevot, A.S.H., Jaffrezo, J.L., Wortham, H., Marchand, N., 2018. Sources of PM2.5 at an urban-industrial Mediterranean city, Marseille (France): Application of the ME-2 solver to inorganic and organic markers. Atmos. Res., 214, 263–274, https://doi.org/10.1016/j.atmosres.2018.08.005.

Sandradewi, J., Prévôt, A.S.H., Weingartner, E., Schmidhauser, R., Gysel, M., Baltensperger, U., 2008. A study of wood burning and traffic aerosols in an Alpine valley using a multi-wavelength Aethalometer. Atmos. Environ., 42, 101–112, https://doi.org/10.1016/j.atmosenv.2007.09.034.

Sandradewi, Jisca, Prévôt, A.S.H., Szidat, S., Perron, N., Alfarra, M.R., Lanz, V.A., Weingartner, E., Baltensperger, U.R.S., 2008. Using aerosol light abosrption measurements for the quantitative determination of wood burning and traffic emission contribution to particulate matter. Environ. Sci. Technol., 42, 3316–3323, https://doi.org/10.1021/es702253m.

Savadkoohi, M., Pandolfi, M., Reche, C., Niemi, J. V, Mooibroek, D., Titos, G., Green, D.C., …, Querol, X., 2023. The variability of mass concentrations and source apportionment analysis of equivalent black carbon across urban Europe. Environ. Int., 178, 108081, https://doi.org/10.1016/j.envint.2023.108081.

Schaap, M., Denier van der Gon, H.A.C., 2007. On the variability of Black Smoke and carbonaceous aerosols in the Netherlands. Atmos. Environ., 41, 5908–5920, https://doi.org/10.1016/j.atmosenv.2007.03.042.

Segersson, D., Eneroth, K., Gidhagen, L., Johansson, C., Omstedt, G., Nylén, A.E., Forsberg, B., 2017. Health impact of PM10, PM2.5 and black carbon exposure due to different source sectors in Stockholm, Gothenburg and Umea, Sweden. Int. J. Environ. Res. Public Health 14, 11–14, https://doi.org/10.3390/ijerph14070742.

Shen, X., Vogel, H., Vogel, B., Huang, W., Mohr, C., Ramisetty, R., Leisner, T., Prévôt, A.S.H., Saathoff, H., 2019. Composition and origin of PM2.5 aerosol particles in the upper Rhine valley in summer. Atmos. Chem. Phys., 19, 20, 13189-13208, https://doi.org/10.5194/acp-19-13189-2019.

Singh, V., Ravindra, K., Sahu, L., Sokhi, R., 2018. Trends of atmospheric black carbon concentration over United Kingdom. Atmos. Environ., 178, 148–157, https://doi.org/10.1016/j.atmosenv.2018.01.030.

Squizzato, S., Masiol, M., Rich, D.Q., Hopke, P.K., 2018. A long-term source apportionment of PM2.5 in New York State during 2005–2016. Atmos. Environ., 192, 35–47, https://doi.org/10.1016/j.atmosenv.2018.08.044.

Srivastava, D., Favez, O., Petit, J. E., Zhang, Y., Sofowote, U. M., Hopke, P. K., Bonnaire, N., Perraudin, E., Gros, V., Villenave, E. and Albinet, A., 2019. Speciation of organic fractions does matter for aerosol source apportionment. Part 3: Combining off-line and on-line measurements, Sci. Total Environ., 690, 944–955, https://doi:10.1016/j.scitotenv.2019.06.378.

Srivastava, D., Tomaz, S., Favez, O., Lanzafame, G.M., Golly, B., Esombes, J.-L., Alleman, L.Y., Jaffrezo, J.-L., Jacob, V., Erraudin, E., Villenave, E., Albinet, A., 2018. Speciation of organic fraction does matter for source apportionment. Part 1: A one-year campaign in Grenoble (France). Sci. Total Environ., 624, 1598-1611, https://doi.org/10.1016/j.scitotenv.2017.12.135.

Thera, B.T.P., Dominutti, P., Öztürk, F., Salameh, T., Sauvage, S., Afif, C., Çetin, B., Gaimoz, C., Keleş, M., Evan, S., Borbon, A., 2019. Composition and variability of gaseous organic pollution in the port megacity of Istanbul: Source attribution, emission ratios, and inventory evaluation. Atmos. Chem. Phys., 19, 23, 15131-15156, https://doi.org/10.5194/acp-19-15131-2019.

Tian, Y., Zhang, Y., Liang, Y., Niu, Z., Xue, Q., Feng, Y., 2020. PM2.5 source apportionment during severe haze episodes in a Chinese megacity based on a 5-month period by using hourly species measurements: Explore how to better conduct PMF during haze episodes. Atmos. Environ., 224, 117364, https://doi.org/10.1016/j.atmosenv.2020.117364.

Titos, G., del Águila, A., Cazorla, A., Lyamani, H., Casquero-Vera, J.A., Colombi, C., Cuccia, E., Gianelle, V., Močnik, G., Alastuey, A., Olmo, F.J., Alados-Arboledas, L., 2017. Spatial and temporal variability of carbonaceous aerosols: Assessing the impact of biomass burning in the urban environment. Sci. Total Environ., 578, 613–625, https://doi.org/10.1016/j.scitotenv.2016.11.007.

Tobler, A. K., Canonaco, F., Skiba, A., Styszko, K., Nęcki, J., Slowik, J. G. and Baltensperger, U., 2021. Characterization and source apportionment of PM 1 organic aerosol in Krakow, Poland, Atmos. Chem., Phys., 21, 14893–14906, https://doi.org/10.5194/acp-21-14893-2021.

Tobler, A., Skiba, A., Wang, D., Croteau, P., Styszko, K., Nęcki, J., Baltensperger, U., Slowik, J. and Prévôt, A.: Improved chloride quantification in quadrupole aerosol chemical speciation monitors (Q-ACSMs), Atmos. Meas. Tech. Discuss., 13, 5293–5301, https://doi.org/10.5194/amt-13-5293-2020.

Tobler, A.K., Skiba, A., Canonaco, F., Močnik, G., Rai, P., Chen, G., Bartyzel, J., Zimnoch, M., Styszko, K., Nęcki, J., Furger, M., Rózański, K., Baltensperger, U., Slowik, J.G., Prevot, A.S.H., 2021. Characterization of non-refractory (NR) PM1and source apportionment of organic aerosol in Kraków, Poland. Atmos. Chem. Phys., 21, 14893–14906, https://doi.org/10.5194/acp-21-14893-2021.

Tomaz, S., Shahpoury, P., Jaffrezo, J.-L., Lammel, G., Perraudin, E., Villenave, E., Albinet, A., 2016. One-year study of polycyclic aromatic compounds at an urban site in Grenoble (France): seasonal variations, gas/particle partitioning and cancer risk estimation. Sci. Total Environ., 565, 1071–1083, https://doi.org/10.1016/j.scitotenv.2016.05.137.

Tong, Y., Qi, L., Stefenelli, G., Wang, D. S., Canonaco, F., Baltensperger, U., ... & Slowik, J. G., 2022. Quantification of primary and secondary organic aerosol sources by combined factor analysis of extractive electrospray ionisation and aerosol mass spectrometer measurements (EESI-TOF and AMS). Atmos. Meas. Tech., 15, 24, 7265-7291. https://doi.org/10.5194/amt-15-7265-2022.

Tremper, Anja H., Anna Font, Max Priestman, Samera H. Hamad, Tsai Chia Chung, Ari Pribadi, Richard J.C. Brown, et al. 2018. Field and Laboratory Evaluation of a High Time Resolution X-Ray Fluorescence Instrument for Determining the Elemental Composition of Ambient Aerosols. Atmos. Meas. Tech., 11, 6, 3541–57, https://doi.org/10.5194/amt-11-3541-2018.

Ulbrich, I. M., Canagaratna, M. R., Zhang, Q., Worsnop, D. R. and Jimenez, J. L., 2009. Interpretation of organic components from Positive Matrix Factorization of aerosol mass spectrometric data, Atmos. Chem. Phys., 9, 9, 2891–2918, https://doi:10.5194/acp-9-2891-2009.

Vanderstraeten, P., Forton, M., Brasseur, O., Offer, Z.Y., 2011. Black Carbon Instead of Particle Mass Concentration as an Indicator for the Traffic Related Particles in the Brussels Capital Region. J. Environ. Prot., 2, 525–532, https://doi.org/10.4236/jep.2011.25060.

Veld M.I., Alastuey A., Pandolfi M., Amato F., Pérez N., Reche C., Via M., Minguillón M.C., Escudero M., Querol X., 2021. Compositional changes of PM2.5 in NE Spain during 2009–2018: A trend analysis of the chemical composition and source apportionment. Sci. Total Environ., 795, 148728, https://doi.org/10.1016/j.scitotenv.2021.148728.

Via, M., Chen, G., Canonaco, F., Daellenbach, K. R., Chazeau, B., Chebaicheb, H., Jiang, J., Keernik, H., Lin, C., Marchand, N., Marin, C., O'Dowd, C., Ovadnevaite, J., Petit, J.-E., Pikridas, M., Riffault, V., Sciare, J., Slowik, J. G., Simon, L., Vasilescu, J., Zhang, Y., Favez, O., Prévôt, A. S. H., Alastuey, A. and Minguillón, M. C., 2022. Rolling vs.

Seasonal PMF: Real-world multi-site and synthetic dataset comparison, EGUsphere, 2022, 1–29 [online] Available from: https://egusphere.copernicus.org/preprints/egusphere-2022-269/.

Via, M., Minguillón, M.C., Reche, C., Querol, X., Alastuey, A., 2021. Increase in secondary organic aerosol in an urban environment. Atmos. Chem. Phys. 21, 8323–8339, https://doi.org/10.5194/acp-21-8323-2021.

Via, M., Yus-díez, J., Canonaco, F., Petit, J., Hopke, P., Reche, C., Pandolfi, M., Ivan, M., Rigler, M., Prev, S. H., Querol, X. and Cruz, M., 2023. Towards a better understanding of fine PM sources: Online and offline datasets combination in a single PMF, Environ. Int., 177, 108006, https://doi:10.1016/j.envint.2023.108006.

Viana, M., Kuhlbusch, T.A.J., Querol, X., Alastuey, A., Harrison, R.M., Hopke, P.K., Winiwarter, W., Vallius, M., Szidat, S., Prévôt, A.S.H., Hueglin, C., Bloemen, H., Wåhlin, P., Vecchi, R., Miranda, A.I., Kasper-Giebl, A., Maenhaut, W., Hitzenberger, R., 2008. Source apportionment of particulate matter in Europe: A review of methods and results. J. Aerosol Sci., 39, 827–849, https://doi.org/10.1016/j.jaerosci.2008.05.007.

Viana, M., M. Pandolfi, M.C. Minguillón, X. Querol, A. Alastuey, E. Monfort, and I. Celades. 2008. Inter-Comparison of Receptor Models for PM Source Apportionment: Case Study in an Industrial Area. Atmos. Environ., 42, 16, 3820–3832, https://doi.org/10.1016/j.atmosenv.2007.12.056.

Virkkula, A., 2021. Modeled source apportionment of black carbon particles coated with a light-scattering shell. Atmos. Meas. Tech., 14, 3707–3719, https://doi.org/10.5194/amt-14-3707-2021.

Wang, Honglei, Qing Miao, Lijuan Shen, Qian Yang, Yezheng Wu, and Heng Wei. 2021. Air Pollutant Variations in Suzhou during the 2019 Novel Coronavirus (COVID-19) Lockdown of 2020: High Time-Resolution Measurements of Aerosol Chemical Compositions and Source Apportionment. Environ. Poll., 271, 116298. https://doi.org/10.1016/j.envpol.2020.116298.

Wang, Q., Qiao, L., Zhou, M., Zhu, S., Griffith, S., Li, L., Yu, J.Z., . 2018. Source Apportionment of PM2.5 Using Hourly Measurements of Elemental Tracers and Major Constituents in an Urban Environment: Investigation of Time-Resolution Influence. J. Geophys. Res: Atmos., 123, 10, 5284–5300, https://doi.org/10.1029/2017JD027877.

Wang, Q., Liu, H., Ye, J., Tian, J., Zhang, T., Zhang, Y., Liu, S., Cao, J., 2021. Estimating Absorption Ångström Exponent of Black Carbon Aerosol by Coupling Multiwavelength Absorption with Chemical Composition. Environ. Sci. Technol. Lett. 8, 121–127. https://doi.org/10.1021/acs.estlett.0c00829.

Watson, J. G., Chow, J. C., & Pace, T. G., 1991. Chemical mass balance. In *Data Handling in Science and Technology* (Vol. 7, pp. 83-116). Elsevier.

Yang, Y., Lou, S., Wang, H., Wang, P. and Liao, H.: Trends and source apportionment of aerosols in Europe during 1980-2018, Atmos. Chem. Phys., 20, 4, 2579–2590, https://doi:10.5194/acp-20-2579-2020, 2020.

Yttri, K.E., Simpson, D., Nojgaard, J.K., Kristensen, K., Genberg, J., Stenström, K., Swietlicki, E., Hillamo, R., Aurela, M., Bauer, H., Offenberg, J.H., Jaoui, M., Dye, C., Eckhardt, S., Burkhart, J.F., Stohl, A., Glasius, M., 2011. Source apportionment of the summer time carbonaceous aerosol at Nordic rural background sites. Atmos. Chem. Phys., 11, 13339–13357, https://doi.org/10.5194/acp-11-13339-2011.

Yu, Y., Shuyan He, S., Wu, X., Zhang, Ch., Yao, Y., Liao, H., Wang, Q., Xie M., 2019. PM2.5 Elements at an Urban Site in Yangtze River Delta, China: High Time-Resolved Measurement and the Application in Source Apportionment. Environ. Poll., 253, 1089–1099, https://doi.org/10.1016/j.envpol.2019.07.096.

Zhan, B., Zhong, H., Chen, H., Chen, Y., Li, X., Wang, L., ... & Chen, J. (2021). The roles of aqueous-phase chemistry and photochemical oxidation in oxygenated organic aerosols formation. Atmospheric Environment, 266, 118738.

Zhang, G., Peng, L., Lian, X., Lin, Q., Bi, X., Chen, D., Li, M., Li, L., Wang, X., Sheng, G., 2019. An improved absorption Ångström exponent (AAE)-based method for evaluating the contribution of light absorption from brown carbon with a high-time resolution. Aerosol Air Qual. Res., 19, 15–24, https://doi.org/10.4209/aaqr.2017.12.0566.

Zhang, X., Mao, M., Chen, H., Tang, S., 2020a. The Angstrom exponents of black carbon aerosols with non-absorptive coating: A numerical investigation. J. Quant. Spectrosc. Radiat. Transf., 257, 107362, https://doi.org/10.1016/j.jqsrt.2020.107362.

Zhang, X., Mao, M., Yin, Y., Tang, S., 2020b. The absorption Ångstrom exponent of black carbon with brown coatings: Effects of aerosol microphysics and parameterization. Atmos. Chem. Phys., 20, 9701–9711, https://doi.org/10.5194/acp-20-9701-2020.

Zhang, Y., Albinet, A., Petit, J.E., Jacob, V., Chevrier, F., Gille, G., Pontet, S., Chrétien, E., Dominik-Sègue, M., Levigoureux, G., Močnik, G., Gros, V., Jaffrezo, J.L., Favez, O., 2020c. Substantial brown carbon emissions from wintertime residential wood burning over France. Sci. Total Environ., 743, https://doi.org/10.1016/j.scitotenv.2020.140752.

Zheng, H., Kong, S., Chen, N., Fan, Z., Zhang, Y., Yao, L., Cheng, Y., Zheng, S., Yan, Y., Liu, D., Zhao, D., Liu, C., Zhao, T., Guo, J., Qi, S., 2021. A method to dynamically constrain black carbon aerosol sources with online monitored potassium. npj Clim. Atmos. Sci., 4, https://doi.org/10.1038/s41612-021-00200-y.

Zhou, L., Hopke, P.K., Paatero, P., Ondov, J.M., Pancras, J.P., Pekney, N.J., Davidson, C. I., 2004. Advanced factor analysis for multiple time resolution aerosol composition data. Atmos. Environ. 38 (29), 4909–4920. https://doi.org/10.1016/j.atmosenv.2004.05.040.

Zografou, O., Gini, M., Manousakas, M. I., Chen, G., Kalogridis, A. C., Diapouli, E., Pappa, A. and Eleftheriadis, K., 2022. Combined organic and inorganic source apportionment on yearlong ToF-ACSM dataset at a suburban station in Athens, Atmos. Meas. Tech., 15, 16, 4675–4692, https://doi:10.5194/amt-15-4675-2022.

Zotter, P., Herich, H., Gysel, M., El-Haddad, I., Zhang, Y., Mocnik, G., Hüglin, C., Baltensperger, U., Szidat, S., Prévôt, A.S.H., 2017. Evaluation of the absorption Ångström exponents for traffic and wood burning in the Aethalometer-based source apportionment using radiocarbon measurements of ambient aerosol. Atmos. Chem. Phys., 17, 4229–4249, https://doi.org/10.5194/acp-17-4229-2017.